Nonlinearity

LONDON MATHEMATICAL SOCIETY EST. 1865

IOP Publishing

PAPER • **OPEN ACCESS**

On the effect of forcing on fold bifurcations and early-warning signals in population dynamics

To cite this article: F Remo *et al* 2022 *Nonlinearity* **35** 6485

View the article online for updates and enhancements.

You may also like

- Slowing Allee effect versus accelerating heavy tails in monostable reaction diffusion equations
Matthieu Alfaro
- WKB theory of large deviations in stochastic populations
Michael Assaf and Baruch Meerson
- A probabilistic cellular automata model for the dynamics of a population driven by logistic growth and weak Allee effect
J R G Mendonça

This content was downloaded from IP address 86.8.136.196 on 06/01/2023 at 14:41

OPEN ACCESS
IOP Publishing | London Mathematical Society Nonlinearity
Nonlinearity **35** (2022) 6485–6527 https://doi.org/10.1088/1361-6544/ac98ee

On the effect of forcing on fold bifurcations and early-warning signals in population dynamics

F Remo[1], G Fuhrmann[2,*] and T Jäger[1]

[1] Institute of Mathematics, Friedrich Schiller University Jena, Germany
[2] Department of Mathematical Sciences, Durham University, United Kingdom

E-mail: flavia.remo@uni-jena.de, gabriel.fuhrmann@durham.ac.uk and tobias.jaeger@uni-jena.de

Received 23 August 2021, revised 13 September 2022
Accepted for publication 10 October 2022
Published 7 November 2022

Abstract

The classical fold bifurcation is a paradigmatic example of a critical transition. It has been used in a variety of contexts, including in particular ecology and climate science, to motivate the role of slow recovery rates and increased auto-correlations as early-warning signals of such transitions. We study the influence of external forcing on fold bifurcations and the respective early-warning signals. Thereby, our prime examples are single-species population dynamical models with Allee effect under the influence of either quasiperiodic forcing or bounded random noise. We show that the presence of these external factors may lead to so-called *non-smooth* fold bifurcations, and thereby has a significant impact on the behaviour of the Lyapunov exponents (and hence the recovery rates). In particular, it may lead to the absence of critical slowing down prior to population collapse. More precisely, unlike in the unforced case, the question whether slow recovery rates can be observed or detected prior to the transition crucially depends on the chosen time-scales and the size of the considered data set.

Keywords: non-autonomous bifurcation theory, strange non-chaotic attractors, non-smooth bifurcations, Allee effect, finite-time Lyapunov exponents

Mathematics Subject Classification numbers: 92D25, 37C60, 34C23.

(Some figures may appear in colour only in the online journal)

*Author to whom any correspondence should be addressed.
Recommended by Dr Hinke M Osinga.

Original content from this work may be used under the terms of the Creative Commons Attribution 3.0 licence. Any further distribution of this work must maintain attribution to the author(s) and the title of the work, journal citation and DOI.

Contents

1. Introduction and overview 6486
1.1. Background and motivation 6487
1.2. The forced Allee model 6488
1.3. The main observation: appearance of a Lyapunov gap 6489
1.4. Mathematical setting and existing results on skew product flows and non-smooth fold bifurcations 6493
1.4.1. Skew product flows 6493
1.4.2. Non-smooth fold bifurcations 6494
1.5. Presentation and discussion of the main results 6495
1.5.1. Lyapunov gap in non-smooth fold bifurcations 6495
1.5.2. Critical slowing down and finite-time Lyapunov exponents 6496
1.5.3. Numerical analysis 6498
1.5.4. Further remarks 6500
1.5.5. Structure of the article 6501
2. Preliminaries 6501
2.1. Skew product flows and invariant graphs 6501
2.2. Fold bifurcation scenario 6504
2.3. Forcing processes 6506
2.4. Application to the forced Allee model 6507
2.5. A simplified discrete-time model 6509
3. Abundance of nonsmooth fold bifurcations 6513
3.1. Quasiperiodic forcing 6513
3.2. Random forcing 6515
4. Lyapunov exponents in nonsmooth fold bifurcations 6518
4.1. Lyapunov gap in nonsmooth fold bifurcations 6518
4.2. Slope at the bifurcation point 6519
5. Range of finite-time Lyapunov exponents 6523
Acknowledgments 6525
References 6525

1. Introduction and overview

In recent years, the notions of *tipping points* and *critical transitions* have received widespread attention throughout a broad scope of sciences. These terms usually refer to abrupt and drastic changes in a system's behaviour upon a small and slow variation of the system parameters [vNS12, Sch09, K11, SCL+12]. In this context, an important issue of immediate practical interest is that of early warning signals, that is, indicators which allow to anticipate an oncoming transition in a systems qualitative behaviour before it actually occurs.

Our aim here is to perform a mathematically rigorous case study of one paradigmatic example of a critical transition—namely the classical fold bifurcation—concerning its

behaviour under the influence of external forcing by quasiperiodic or random processes. It turns out that such external factors can have a significant impact on possible early warning signals. In order to demonstrate our findings and to compare them with numerical results, we focus on the well-known Allee model from population dynamics.

Naturally, a topic of such general interest and possible practical applications like that of critical transitions can be studied by a variety of different and inter-disciplinary approaches. Consequently, a wide range of experts, including physicists, biologists, ecologists, climate scientists and many others have made important contributions to the area. For mathematicians, such as the authors of this article, this poses the particular challenge of presenting results in a way that is accessible to a wide audience without losing the mathematical precision. In order to find a hopefully good balance between these two objectives, we will use this introductory chapter to first give a complete overview of the article, which includes not only the background and motivation of the main model and key concepts, but also a brief introduction of the mathematical setting we use and a discussion of the main results. The mathematical details and the rigorous proofs of these results are then provided in the later chapters. A short outline of the overall structure of the article is given at the end of this introduction.

1.1. Background and motivation

A concept that has led to widely recognised advances concerning early warning signals of critical transitions are *slow recovery rates* (also referred to as *critical slowing down*), which often come along with an *increase in autocorrelation* [vNS12, SBB+09, Sch09, SCL+12, VFD+12]. Both have been described as possible early warning signals in a variety of contexts, in theoretical as well as in experimental settings [DSvN+08, CCP+11, GJT13, vLWC+14, KGB+14, RDB+16].

Roughly speaking, the *recovery rate* of a system '*in equilibrium*' is the speed with which it returns to this equilibrium after a perturbation. *Slow recovery rates* or *critical slowing down* then refers to the fact that these recovery rates are equal or converge to zero, which may happen for instance during a critical transition. *Autocorrelation* is a term that is usually defined in the context of stationary stochastic processes and time series analysis and refers to the correlation between a time-dependent observable X_t at time t and a lagged version X_{t-k}. It should be emphasized, however, that in the context critical transitions all these notions (including the term '*critical transition*' itself) are usually used in a non-mathematical sense and do not have a precise mathematical definition.[3] The reason for this is the fact that on the one hand all these terms may refer to a variety of different phenomena or situations, and on the other hand even the same phenomenon or real-world process may be modeled by very different mathematical methods, ranging from autonomous and non-autonomous dynamical systems to random or stochastic differential equations, compartmental models and others. This makes it difficult to provide a common mathematical framework and precise and comprehensive definitions of the above notions—an issue which is well-known in non-linear dynamics and comes up in similar form for key concepts like 'chaos', 'fractals' or 'strange attractors' in dynamical systems theory. However, since we restrict ourselves to the study of one particular model and in this specific context recovery rates—on which our focus will lie—can be captured by the mathematical concept of (asymptotic or finite-time) Lyapunov exponents, we will not be concerned with this problem.

[3] This even refers to '*autocorrelation*' whenever this notion used in a non-stationary context, where the extension of the definition for stationary processes is difficult.

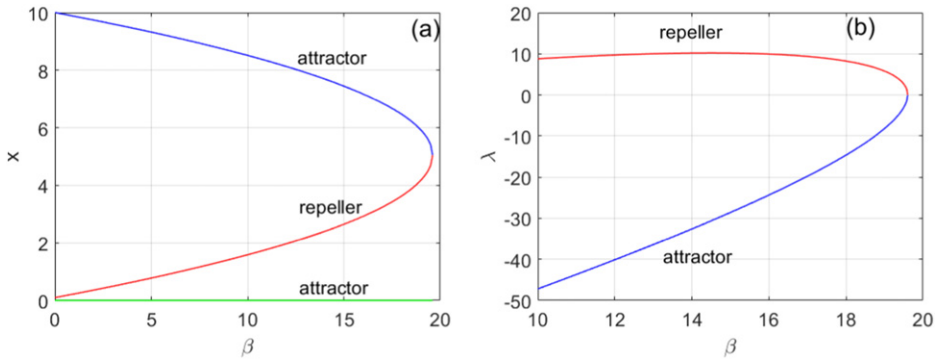

Figure 1. (a) Bifurcation diagram of a fold bifurcation in the Allee model (1) with parameters $r = 80, K = 10, S = 0.1$ and a bifurcation at a critical parameter $\beta_c \simeq 19.978$. The stable non-zero equilibrium is shown in blue, the unstable equilibrium in red. The stable equilibrium at $x = 0$ is shown in green. (b) Behaviour of the Lyapunov exponents of the upper stable and the unstable equilibrium during the fold bifurcation. Note that in this situation, the Lyapunov exponents coincide with the value of the derivative v'_β of the right-hand side of (1) at the respective equilibria.

1.2. The forced Allee model

The situation we will concentrate on is the classical fold bifurcation, which comprises key features of critical transitions and has emerged as a paradigmatic example in this context [Sch09]. As it is well-known, in this type of bifurcation a stable and an unstable equilibrium point of a parameter-dependent scalar ODE approach each other and eventually merge to form a single neutral equilibrium point, which then vanishes. Since this leads to the disappearance of all equilibria in a certain region, it presents the abrupt change in the system's qualitative behaviour that is characteristic of critical transitions. In order to fix ideas, we consider as a specific example the single-species population model with Allee effect given by the scalar ODE

$$\begin{aligned} x' &= rx \cdot \left(1 - \frac{x}{K}\right) \cdot \left(\frac{x}{K} - \frac{S}{K}\right) - \beta x \\ &= \frac{r}{K^2} \cdot x \cdot (K - x) \cdot (x - S) - \beta x \;=:\; v_\beta(x) \end{aligned} \tag{1}$$

Here $r > 0$ denotes the intrinsic growth factor of the population, $K > 0$ is the carrying capacity and $S \in (0, K)$ is the threshold value below which the population dies out due to an Allee effect. The term βx represents an external stress factor that puts additional pressure on the population. An increase of the parameter β leads to a fold bifurcation and the subsequent collapse of the population at some critical value $\beta_c > 0$.[4] The bifurcation pattern is drawn in figure 1(a), whereas figure 1(b) shows the behaviour of the Lyapunov exponents of the attracting and repelling equilibria during the bifurcation.

In this setting, one obvious possible mathematical interpretation of *recovery rates* is to identify them with the Lyapunov exponents of the stable or neutral equilibria, so that *slow recovery*

[4] In fact, a straightforward calculation yields $\beta_c = \frac{(K-S)^2 \cdot r}{4K^2}$.

rates and *critical slowing down* correspond exactly to the fact that the Lyapunov exponents in figure 1(b) (and in particular the one at the stable equilibrium) go to zero as the bifurcation parameter is approached.

Our main goal is to investigate fold bifurcations in forced versions of the autonomous Allee model (1), which are given by a non-autonomous scalar ODE of the form

$$x'(t) = \frac{r}{K^2} \cdot x(t) \cdot (K - x(t)) \cdot (x(t) - S) - (\beta + \kappa \cdot F(t)) \cdot x \tag{2}$$

Here, time-dependence (or external forcing) of the system (2) is introduced via a *forcing term* $\kappa \cdot F(t)$, with *coupling constant* $\kappa > 0$ and a forcing function $F : \mathbb{R} \to [0, 1]$. We consider two different types of forcing processes.

Quasiperiodic forcing: this kind of forcing corresponds to the influence of several periodic external factors with incommensurate frequencies $\rho_1, \ldots, \rho_d \in \mathbb{R}$. As a specific example, we choose the forcing function as

$$F(t) = \prod_{i=1}^{d} \left(\frac{1 + \sin(2\pi(\theta_i + t \cdot \rho_i))}{2} \right)^q, \tag{3}$$

with arbitrary initial conditions $\theta_1, \ldots, \theta_d \in \mathbb{R}$. Let us note here that due to the periodicity of the sine function, these initial values may also be viewed as elements of the circle $\mathbb{T}^1 = \mathbb{R}/(2\pi\mathbb{Z})$ so that $\theta = (\theta_1, \ldots, \theta_d)$ becomes an element of the d-torus $\mathbb{T}^d = \mathbb{R}^d/(2\pi\mathbb{Z})^d$. The parameter $q \in \mathbb{N}$ allows some additional control of the geometry of the forcing function.

Bounded random noise: secondly, we consider the effect of external random perturbations on the system, given by the forcing function

$$F(t) = \frac{1 + \sin(\theta_0 + W_t)}{2}, \tag{4}$$

where $\theta_0 \in \mathbb{T}^1$ is again an arbitrary initial condition and W_t denotes a one-dimensional Brownian motion (but higher-dimensional analogues could be considered as well).

We thus arrive at the forced scalar differential equation (2), with the forcing function F given either by (3) or (4), as basic models on which we put our main focus throughout this introduction. Thereby, we will refer to the equation (2) with forcing term given by (3) as the *quasiperiodically forced (qpf) Allee model*, and to (2) with forcing term (4) as the *randomly forced (rdf) Allee model*. Most of the statements we actually prove in the later sections hold in greater generality, both with respect to the model (2) and to the employed forcing processes (3) and (4). In some other cases, we will need to replace the Allee model by discrete time systems with qualitatively similar behaviour in order to obtain rigorous results. These systems should then be considered as simplified models for the time-one-maps or Poincaré return maps of the flow induced by (2). However, we refer to the respective later sections for details in order to avoid too many technicalities at this point.

1.3. The main observation: appearance of a Lyapunov gap

In order to discuss what happens with the fold bifurcation pattern and the corresponding early-warning signals in the forced Allee model (2), we will first concentrate on the behaviour of the Lyapunov exponents. Figure 2 shows the behaviour of the Lyapunov exponents of the attractor and the repeller of (2) throughout the bifurcation, with two different choices of the parameters κ and q in the case of quasiperiodic forcing in (a) and (b) and different parameters κ in the random case in (c) and (d).

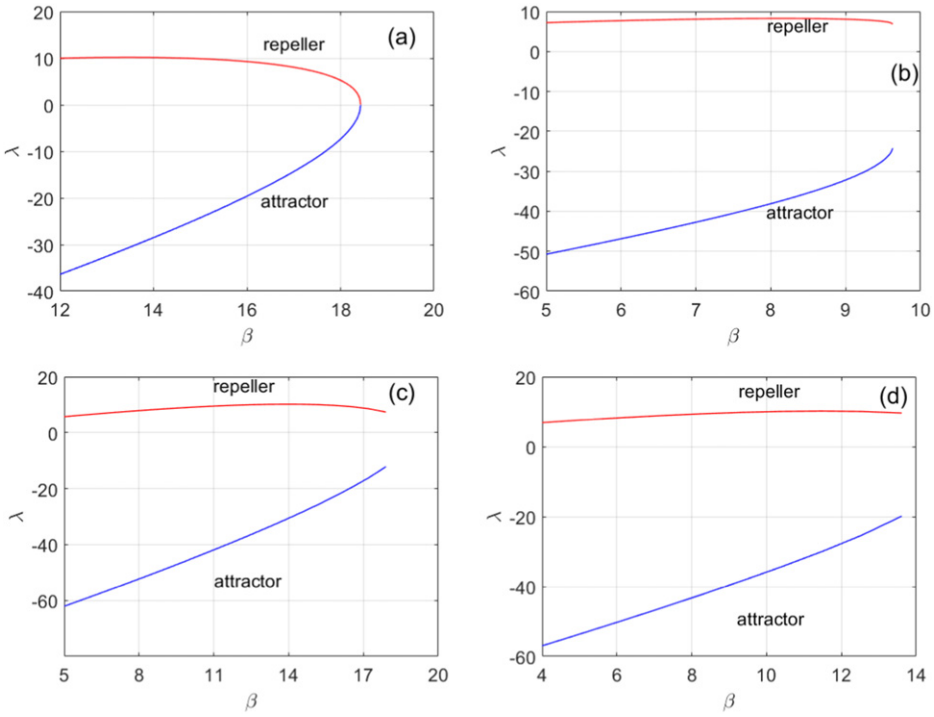

Figure 2. (a) and (b) Lyapunov exponents during fold bifurcations in the qpf Allee model (2) with forcing term (3); (a) smooth bifurcation with $r = 80, K = 10$, $S = 0.1, q = 1, \nu = (2\omega, 2\pi)$ (where ω is the golden mean) and $\kappa = 4$ (bifurcation at $\beta_c \simeq 18.4269$); (b) non-smooth bifurcation with $r = 80, K = 10, S = 0.1, q = 5$, $\nu = (2\omega, 2\pi)$ and $\kappa = 51.2$. The bifurcation occurs at $\beta_c \simeq 9.628$. (c) and (d) Lyapunov exponents during the fold bifurcation in the rdf Allee model (2) with forcing term (4); (c) with $r = 80, K = 10, S = 0.1, \kappa = 2$ and bifurcation parameter $\beta_c = 17.978$; (d) with $r = 80, K = 10, S = 0.1, \kappa = 6$ and bifurcation parameter $\beta_c = 13.978$.

While the behaviour in (a) is in analogy to the unforced case in figure 1(b), the situation in (b)–(d) is clearly different. Although the Lyapunov exponents of the attractor and the repeller do approach each other, there remains a clear gap at the bifurcation point, and in particular the Lyapunov exponents of the attractor (which are the 'visible' or 'physically relevant' ones) stay strictly away from zero. Given the significance of zero exponents for the observation of critical slowing down and slow recovery rates, this is certainly noteworthy and deserves a closer examination. Moreover, while in figures 2(b)–(d) the Lyapunov exponents do at least move towards each other as the bifurcation is approached, this actually turns out to depend just on the precise form of the parameter family. In all cases shown in figure 2, we have only varied the bifurcation parameter β, while leaving all other constants invariant. In contrast to this, it seems likely that in real-world situations other system parameters, such as the intrinsic growth rate r in (2) or the noise amplitude in (4), vary as well as the pressure on the population increases. The result of such couplings is shown in figure 3. It can be seen that in this case the Lyapunov exponents may move away from each other all throughout the bifurcation process, and hence there is no chance at all to anticipate the oncoming transition based only on their behaviour.

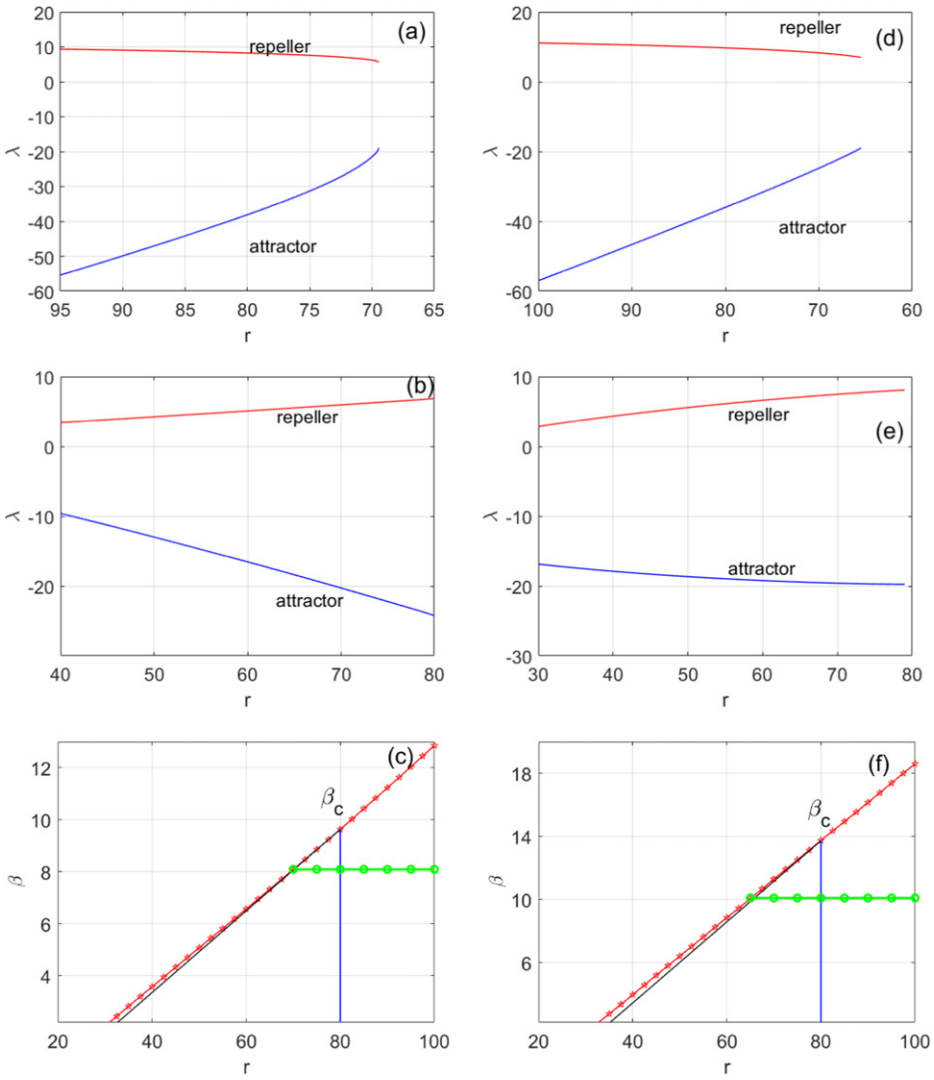

Figure 3. Lyapunov exponents during fold bifurcations in the forced Allee model with different variations of parameters. (a) Shows the behaviour in the qpf case as the parameter r is decreased, corresponding to the horizontal green line in the two-parameter space depicted in (c). In contrast, (b) shows the behaviour when β and r are varied simultaneously along the black curve in (c). In this case, the Lyapunov exponents move apart throughout the entire bifurcation process. In (d) and (e), similar plots are shown for the rdf case. In (d), again only the parameter r is varied and decreases along the horizontal green line in (f). In (e), both parameters β and r are again varied at the same time, along the black curve in (f). In both (c) and (f), the red line is an interpolation of the numerically determined critical parameters for different values of β and r. The vertical blue line in (c) and (f) just connects the intersection point of the black parameter curve and the red curve of bifurcations parameters with the horizontal axis, showing that the intersection takes place exactly at $r = 80$.

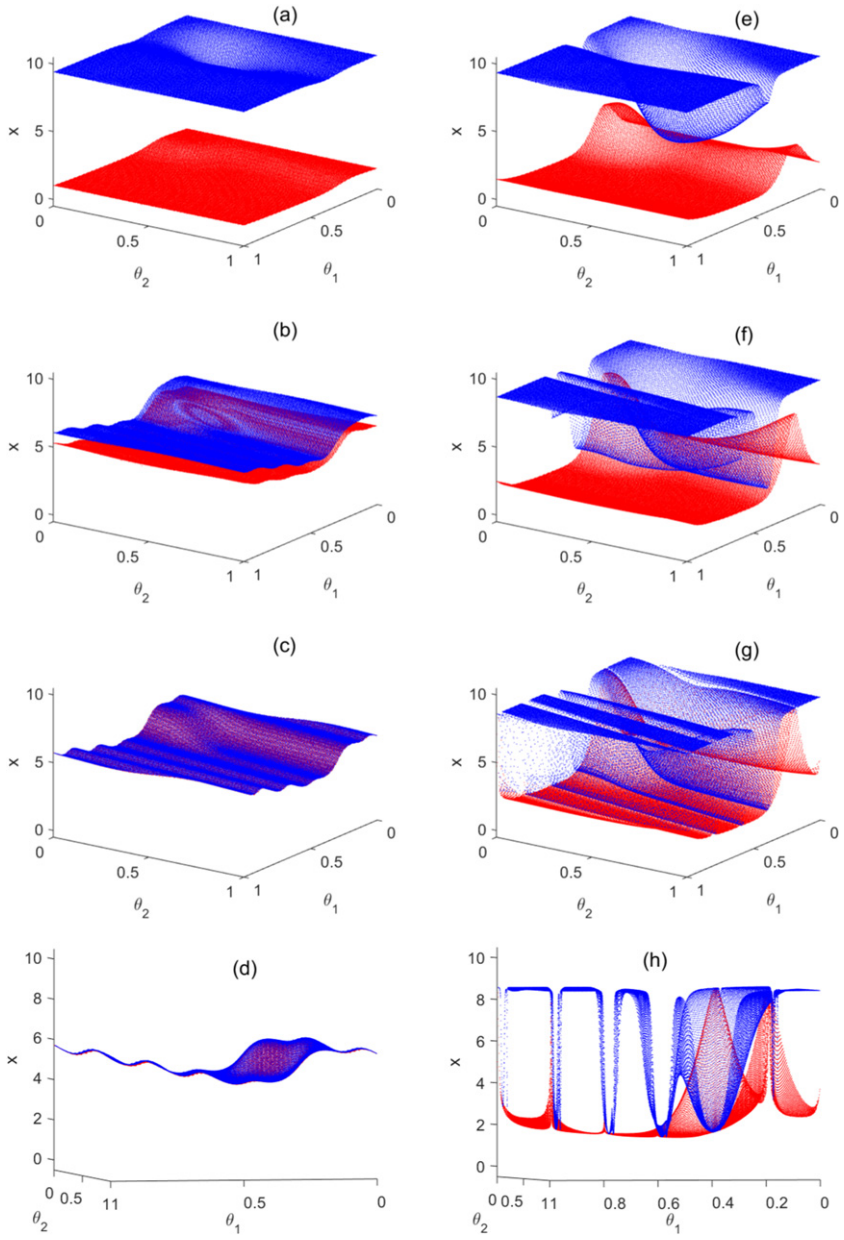

Figure 4. (a)–(d) Smooth fold bifurcation in the qpf Allee model with parameters $r = 35, K = 10, S = 0.1, q = 3$ and $\kappa = 41$ and $\beta = 2$ in (a), $\beta = 7.8$ in (b) and $\beta = 7.8455$ in (c) and (d). The attractor is shown in blue, the repeller in red. The last two figures show the merged attractor and repeller at the bifurcation point from two different angles. The rotation vector ρ is $\rho = (5\omega, 5\pi)$ in all cases, where ω is the irrational part of the golden mean. (e)–(h) Non-smooth fold bifurcation in the qpf Allee model with parameters $r = 80$, $K = 10$, $S = 0.1$, $q = 5$ and $\kappa = 51.2$ and $\beta = 2$ in (e), $\beta = 9$ in (f) and $\beta = 9.6282$ in (g) and (h). Again the last two figures show the attractor (blue) and the repeller (red) at the bifurcation point from two different angles. The rotation vector ρ is $\rho = (2\omega, 2\pi)$.

Remark 1.1. We should note that the phenomena that we describe here are known by folklore in the field of stochastic processes and stochastic differential equations, where the presence of noise equally prevents the recovery rates from going down all the way to zero before a transition happens. However, in this context it is much harder to pin this observation down mathematically, since the presence of unbounded noise immediately 'destroys' the fold bifurcation and leads to the existence of a unique stationary measure in stochastic versions of (2) and similar models. Moreover, the forcing with bounded noise is arguably quite relevant and intrinsically motivated from the biological and population dynamical viewpoint, since reproduction rates are certainly bounded.

1.4. Mathematical setting and existing results on skew product flows and non-smooth fold bifurcations

1.4.1. Skew product flows. In order to understand and explain these phenomena, it is indispensable to have a look at the mathematical framework that we will use to describe fold bifurcations in forced systems. To that end, we first concentrate on the case of quasiperiodic forcing. The rigorous analysis of non-autonomous ODE's, such as the one given by (2) and (3), hinges on the fact that the family of equation (2), with all possible initial conditions $\theta = (\theta_1, \dots, \theta_d) \in \mathbb{T}^d$, defines a skew product flow

$$\Xi : \mathbb{R} \times \Theta \times \mathbb{R} \to \Theta \times \mathbb{R}, \quad (t, \theta, x) \mapsto \Xi^t(\theta, x) = (\omega_t(\theta), \xi^t(\theta, x)). \tag{5}$$

Here, the *driving space* Θ is the d-torus $\Theta = \mathbb{T}^d = \mathbb{R}^d/\mathbb{Z}^d$ (corresponding to the set of possible initial conditions). The *driving flow* $\omega : \mathbb{R} \times \Theta \to \Theta$ is given by the irrational Kronecker flow $\omega_t(\theta) = \theta + t \cdot \rho$ with translation vector[5] $\rho = (\rho_1, \dots, \nu_d)$, and models the quasiperiodic dynamics of the external driving factors. The flow Ξ is uniquely determined by the fact that the mapping $t \mapsto \xi^t(\theta, x)$ is the solution to (2) with forcing function (3). A similar flow representation can be given in the case of random forcing. We will describe this passage from non-autonomous equations to skew product flows in more detail in section 2.1, but also refer the mathematically interested reader to standard references such as [Arn98, HY09] for further reading.

Remark 1.2. We note that the solutions of (2), with forcing terms (3) or (4), are always defined for all $t \geqslant 0$. The reason for this is the fact that the right side of the differential equation (2) is cubic in x, with negative leading term $-(r/K^2) \cdot x^3$ and the dependence on t, given by $-\kappa F(t) \cdot x$, is uniformly bounded since $0 \leqslant F(t) \leqslant 1$. For this reason, all solutions $x(t)$ eventually enter and remain in a compact interval $A \subseteq \mathbb{R}$. This prevents solutions from escaping to infinity and ensures their existence for all $t \in \mathbb{R}^+$.

For negative times $t < 0$, this is different. In fact, any solution starting far enough from the origin ($|x_0|$ large) will escape to $\pm\infty$ in finite negative time, since for $t \to -\infty$ such solutions will behave qualitatively like the solutions $y(t) = 1/\sqrt{2t + y_0^{-2}}$ of $y' = -y^3$.

However, as it will turn out in the course of our analysis, for the description of non-smooth fold bifurcations in models like (2) it suffices to consider those solutions which are globally defined and remain bounded in the interval $[0, K]$ at all times. The reason is the fact that this is where the bifurcating objects—which are invariant graphs or random fixed points/equilibria

[5] Composed of the d incommensurate frequencies ρ_i in (3).

defined below (see also section 2.1)—are located and the actual bifurcations take place. Therefore, one could modify the right side of (2) on $\mathbb{R} \times (\mathbb{R}\backslash[0, K])$ in such a way that this function becomes uniformly bounded, and thus induces a flow with globally defined solutions. This will not affect any solutions starting on the invariant graphs/random equilibria, since such solutions remain bounded for all times, and thus has no effect on the bifurcation.

Hence, for the sake of simplicity and an easier notation, we will in general assume that skew product flows of the form (5) are well-defined on all of $\mathbb{R} \times \Theta \times \mathbb{R}$.

The advantage of the skew product setting lies in the fact that the classical notion of equilibrium points—which does not make sense anymore for time-dependent systems such as (2)—can be replaced by that of *random* or *non-autonomous equilibria*. These are defined as measurable functions $x : \Theta \to \mathbb{R},\ \theta \mapsto x(\theta)$ that satisfy $\Xi^t(\theta, x(\theta)) = x(\omega_t(\theta))$. Hence, a non-autonomous equilibrium can be thought of as a curve, surface or higher-dimensional submanifold of the product space $\Theta \times \mathbb{R}$ that can be represented as a graph over the base space Θ, is invariant under the skew product flow Ξ and is composed of solutions of (2) with varying initial conditions. With this new notion of an equilibrium, fold bifurcations in forced systems can be described, in analogy to the classical case, as the collision and subsequent extinction of a stable and an unstable equilibrium [NO07, AJ02]. This process is shown in figures 4(a)–(d) where two such equilibrium manifolds approach each other and then merge to form a neutral equilibrium.

1.4.2. Non-smooth fold bifurcations. In contrast to the unforced case, however, there is a second possibility how such a collision can occur. As the value of the non-autonomous equilibria depend on the forcing variable θ, the two curves or surfaces can also collide only for some values of θ, without merging together uniformly. This pattern is shown in figures 4(e)–(h). In this case, one speaks of a *non-smooth fold bifurcation*, in which the neutral equilibrium at the bifurcation point is replaced by an attractor-repeller pair (where the attractor is characterised by a negative and the repeller by a positive Lyapunov exponent). Moreover, in the case of quasiperiodic forcing the stable and unstable non-autonomous equilibria are called *strange non-chaotic attractors (SNA)* and *strange non-chaotic repellers (SNR)* due to their unusual combination of a fractal geometry and non-chaotic dynamics [GOPY84, Bje05, FKP06, HP06, Jäg09, Fuh16a, FGJ18]. For a precise mathematical definition of these notions, we refer to section 2.2 (in particular theorem 2.2). It is this dichotomy between smooth and non-smooth fold bifurcations which causes the different behaviour of the Lyapunov exponents observed in figure 2.

Before we make this precise, in theorem 1 below, it seems fit to comment on the relevance of non-smooth bifurcations. An immediate question that can be asked is whether this alternative form of the fold bifurcation in forced systems present a very common phenomenon, or if it is rather 'pathological' and may not play an important role for the description of real-world processes. However, in the case of quasiperiodic forcing, the wide-spread occurrence of non-smooth bifurcations and the related existence of SNA has been observed in a large number of numerical and experimental studies and in a variety of different contexts, ranging from classical and electronic oscillators to quantum mechanics, conceptual climate models and astrophysics (e.g. [RBO+87, DRC+89, WFP97, VLPR00, HP06, MCA15, RRM15, Zha13, LKK+15]). In addition, the simulations in figures 2(b) and 4(e)–(h) provide similar numerical evidence for the existence of nonsmooth bifurcations in the qpf Allee model (2) and (3). These findings are backed up by rigorous results in [Fuh16a, FGJ18, Fuh16b], showing that non-smooth fold bifurcations occur for open sets of parameter families of qpf scalar ODE's. They can therefore be robust and persistent under small perturbations of the system. In the light of these results, one may say that fold bifurcations in qpf models may be either smooth or non-smooth, depending

on the precise form of the model and the shape and strength of the forcing, and both of the cases are sufficiently widespread and persistent to be relevant in practical considerations and applications. As for the case of random forcing, according to our knowledge the phenomenon of non-smooth bifurcations has not been studied previously. However, at least in the specific situation of the rdf Allee model given by (2) and (4), theorem 2 below demonstrates as well that the non-smooth case is far from exceptional.

In the existing literature, non-smooth fold and saddle-node bifurcation have mainly been discussed in the context of strange non-chaotic attractors, since they present one of the main mechanisms for the creation of these objects. There exists a vast amount of numerical studies on this topic, which has attracted considerable attention in computational and theoretical physics since the early 1990's, in the physics literature. We refrain from going into detail and refer to the monograph [FKP06] for an overview and further references. The mathematical literature on the subject is far more restricted. The first rigorous proof for the occurrence of non-smooth saddle-node bifurcations has been given in [Her83] for a particular discrete-time model that is related to one-dimensional Schrödinger operators with quasiperiodic potential. A more detailed study of these models under more general assumptions has been performed later in [Bje05, Bje05b, Bje07], whereas results on some new model classes, but under somewhat restrictive conditions, have been established in [Jäg09]. The combination of these methods then allowed to extend these proofs to more general classes of qpf systems in the above-mentioned work [Fuh16a, FGJ18, Fuh16b]. Apart from that, a general setting for fold bifurcations has been provided in [NO07] for minimally forced systems and in [AJ02] for more general classes of forcing processes.

1.5. Presentation and discussion of the main results

1.5.1. Lyapunov gap in non-smooth fold bifurcations. In order to give a precise description of the connection between non-smooth fold bifurcations and the Lyapunov gap, we denote by x^{s}_β the non-zero stable equilibrium of (2) at parameter β,[6] and by $\lambda(x^{\mathrm{s}}_\beta)$ its associated Lyapunov exponent. We refer again to section 2 for the precise definitions. In order to obtain rigorous results, we will need to apply a general framework for non-autonomous fold and saddle-node bifurcations that has been established in [AJ02] and will be discussed in detail in section 2.2. For the moment, we only need to mention that an important condition for the application of these results is the concavity of the fibre maps in the region where the bifurcation takes place. This is, in turn, a consequence of the concavity of the right side of the respective non-autonomous ODE. In order to ensure this concavity in (2), we need to restrict to suitable parameter ranges, as specified in the following.

Remark 1.3. We let

$$b(r,K,S)=\frac{r}{K^2}\cdot\left(\frac{K-S}{2}\right)^2 \quad \text{and} \quad \gamma(K,S)=\frac{1}{9}\cdot\left(\frac{K+S}{K-S}\right)^2 \tag{6}$$

and assume that

$$\kappa \;<\; b(r,K,S)\cdot(1-\gamma(K,S)). \tag{7}$$

[6] Note that there is always an equilibrium at zero, which is a natural requirement for any population dynamical model and ensured by the multiplicative form of the forcing in (2). Due to the Allee effect, the zero equilibrium is stable as well and presents the unique global attractor of the system after the bifurcation.

Then, as we explain in detail in section 2.4, the family (2) with forcing term (3) or (4) undergoes a fold bifurcation in the parameter interval

$$J(r,K,S) = [b(r,K,S)\cdot(1-\gamma(K,S)), b(r,K,S)+1]. \tag{8}$$

It should be mentioned, however, that this restriction in the parameter ranges is rather a technical condition and could easily be improved, in particular by using numerical methods, in order to include a broader range of parameters. The crucial condition is that the time-t-maps of skew product flows induced by (2) are concave for some $t > 0$. Hence, even if not all of our examples satisfy condition (7), it seems more reasonable to rely on the numerical evidence for the occurrence of fold bifurcations in these cases than to resort to highly technical proofs that do not add further insight. However, all the rigorous statements provided below will be restricted to the parameter range $J(r,K,S)$.

Theorem 1. *Suppose that* (7) *holds. If the Allee model* (2) *with forcing term given by* (3) *or* (4) *undergoes a non-smooth fold bifurcation at the critical parameter* $\beta_c \in J(r,K,S)$*, then we have that*

$$\lim_{\beta\nearrow\beta_c} \lambda(x^s_\beta) = \lambda(x^s_{\beta_c}) \;<\; 0. \tag{9}$$

If the fold bifurcation is smooth, then we have $\lim_{\beta\nearrow\beta_c} \lambda(x^s_\beta) = 0$*. The analogous results hold for the unstable equilibrium* x^u_β*.*

We prove a more general version of this result, namely theorem 4.1, in section 4.1.

As we have discussed in the previous subsection, whether or not a fold bifurcation in a qpf system is smooth or non-smooth depends on the precise system parameters, and the numerical evidence presented in figures 2 and 4 suggests that both pattern occur for the qpf Allee model. In contrast to this, the following result states that in the case of the rdf Allee model with forcing term (4) only non-smooth bifurcations occur.

Theorem 2. *Suppose that* (7) *holds. Then any fold bifurcation that occurs in the forced Allee model* (2) *with random forcing term* (4) *at a critical parameter* $\beta_c \in J(r,K,S)$ *is non-smooth.*

This statement is a direct consequence of the more general theorem 3.4, which is stated and proven in section 3.2.

1.5.2. Critical slowing down and finite-time Lyapunov exponents. The interpretation of the Lyapunov gap in a non-smooth fold bifurcation depends on the precise meaning given to the notion of recovery rates. If these are identified with the Lyapunov exponents, then it follows that, unlike in classical fold bifurcations, there are no slow recovery rates in non-smooth fold bifurcations. However, it would also seems reasonable to say that the intuitive meaning of recovery rates, as used in experimental studies like [SBB+09], is better captured by the mathematical notion of *finite time Lyapunov exponents*. Instead of measuring the asymptotic stability of an orbit, these only take into account the expansion or contraction around an orbit over some finite time span. Given $T > 0$, we denote the Lyapunov exponent at time T of the flow generated by (2) and starting at an initial condition $(\theta, x) \in \Theta \times \mathbb{R}$ by $\lambda_T(\theta, x)$.

In a smooth fold bifurcation, it is known that all finite time Lyapunov exponents in the basin of attraction of the stable equilibrium x^s_β will be very close to $\lambda(x^s_\beta)$, provided the time T is sufficiently large [SS00]. In contrast to this, the non-smooth case shows a characteristic spreading of these quantities, which can be observed in figure 5.

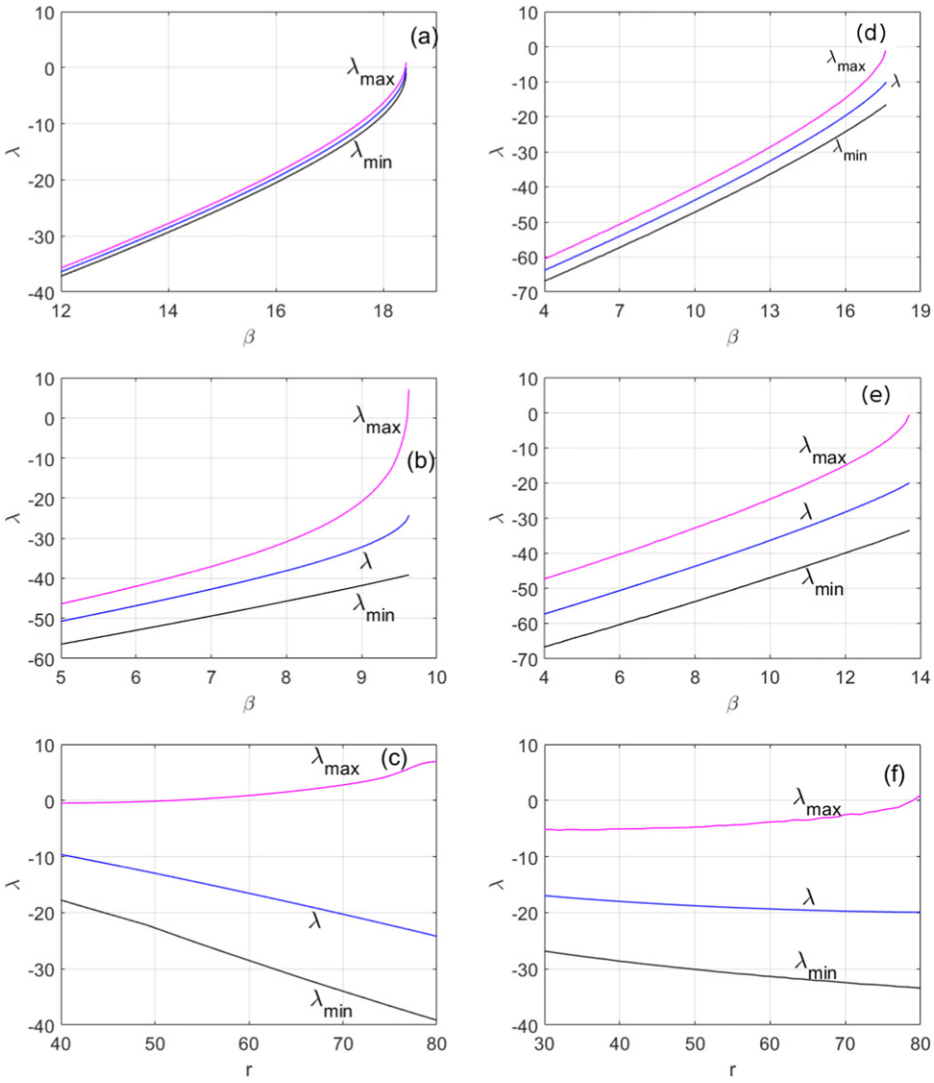

Figure 5. The above plots (a)–(f) show the behaviour of the finite-time Lyapunov exponents during fold bifurcations in the forced Allee model. The middle curve is always the time 2000 Lyapunov exponent (as an approximation of the asymptotic Lyapunov exponent), whereas the upper and the lower curves correspond to the maximal and minimal time 4/3 Lyapunov exponents, respectively. (a) Shows the case of a smooth fold bifurcation in the qpf Allee model with parameter values $r = 80, K = 10, S = 0.1, \kappa = 4$ and $q = 1$. (b) Shows the case of a nonsmooth fold bifurcation in the same model with $r = 80, K = 10, S = 0.1, \kappa = 51.2$ and $q = 5$. (c) Shows a quasiperiodic case again, but this time with the simultaneous variation of parameters depicted in the black line, as in figure 3(c). (d) and (e) Show the case of a non-smooth fold bifurcation in the randomly forced Allee model with parameters $r = 80, K = 10, S = 0.1$ and $\kappa = 2$ and $\kappa = 6$, respectively. Finally, (f) shows the random case simultaneous variation of parameters as in figure 3(f).

In order to translate this observation into a rigorous statement, we denote the largest time T Lyapunov exponents that is 'observable' on the attractor x^{s}_{β} by $\lambda^{\max}_{t}(x^{\mathrm{s}}_{\beta})$, the minimal one by $\lambda^{\min}(x^{\mathrm{s}}_{\beta})$. (We refer to section 5 for the precise definition.) The behaviour differs according to whether the forcing is quasiperiodic or random.

Theorem 3. *Suppose that* (7) *holds. If the forced Allee model* (2) *with quasiperiodic forcing term* (3) *undergoes a non-smooth fold bifurcation at some critical parameter* $\beta_{\mathrm{c}} \in J(r, K, S)$, *then we have that for any* $T > 0$

$$\lim_{\beta \nearrow \beta_{\mathrm{c}}} \lambda^{\max}_{T}(x^{\mathrm{s}}_{\beta}) \geqslant \lambda(x^{\mathrm{u}}_{\beta_{\mathrm{c}}}) \; > \; 0, \tag{10}$$

$$\lim_{\beta \nearrow \beta_{\mathrm{c}}} \lambda^{\min}_{T}(x^{\mathrm{u}}_{\beta}) \leqslant \lambda(x^{\mathrm{s}}_{\beta_{\mathrm{c}}}) \; < \; 0. \tag{11}$$

In the case of random forcing (4), *we have that for any* $T \geqslant 0$

$$\lim_{\beta \nearrow \beta_{\mathrm{c}}} \lambda^{\max}_{T}(x^{\mathrm{s}}_{\beta}) \; \geqslant \; 0. \tag{12}$$

This result is a direct consequence of theorem 5.1 (for the qpf case) and theorem 5.3 (for the rdf case), which are stated and proven in section 5.

Both the statement and the numerical results imply that at least in theory non-smooth fold bifurcations can be anticipated and detected beforehand via a spread in the distribution of finite-time Lyapunov exponents, which reaches into the positive region. However, at the same time this highlights a variety of practical problems that may arise when trying to establish early-warning signals for forced systems on the basis of recovery rates. Unlike for Lyapunov exponents, which are asymptotic quantities and usually show a very uniform behaviour, the use of finite-time Lyapunov exponents requires to make a number of choices. First of all, there is the question of the time-scale (the choice of T) for which these quantities should be measured. When T is too small, it is likely that positive finite-time exponents will be observed already far from any bifurcation (depending on the geometry of the system). Conversely, if T is chosen too large, positive finite-time exponents may exist, but may only be observed with very small probabilities (thus requiring many measurements for a reliable signal). In any case, even with the right choice of the time-scale and sufficient data, examples as the one shown in figure 5(c) will remain difficult to treat.

Finally, at the critical parameter, we take a brief look at the distribution of finite-time Lyapunov exponents on different timescales, which are shown in figure 6 (for the qpf case; for results in the random case, see figure 8). The probability of observing exponents above or close to zero is plotted in figure 7(a) and decreases quickly (see figure 9 for the respective plots in the random case). Our simulations are somewhat inconclusive concerning the rate of decay, which seems to be somewhere between polynomial and exponential. However, exponential decay is confirmed rigorously in [FJR22] for so-called pinched skew products, which are in many aspects very similar to the systems we study here.

1.5.3. Numerical analysis. We throughout illustrate the findings of this article with numerical experiments. The numerical analysis of the studied systems is greatly simplified by the fact that equilibria with negative Lyapunov exponents are attracting in forward time (hence the name *attractor*), while an equilibrium with positive Lyapunov exponent (a so-called *repeller*) is attracting in backward time, see also section 2. Accordingly, to study a certain property of

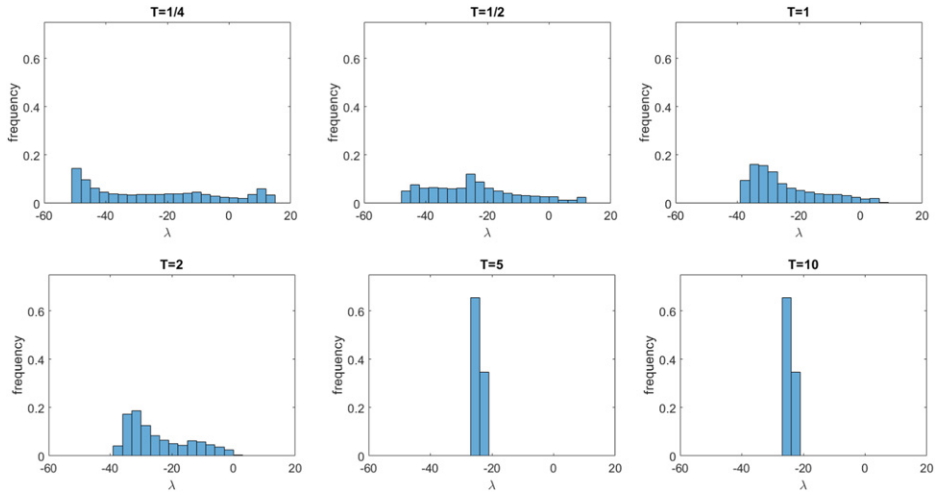

Figure 6. Distributions of the finite-time Lyapunov exponents in the qpf Allee model (2) with parameters $r = 80$, $K = 10$, $S = 0.1$, $\kappa = 51.2$ and $\beta = 9.629$ on different timescales, computed with sliding windows over a trajectory of length $t = 20\,000$.

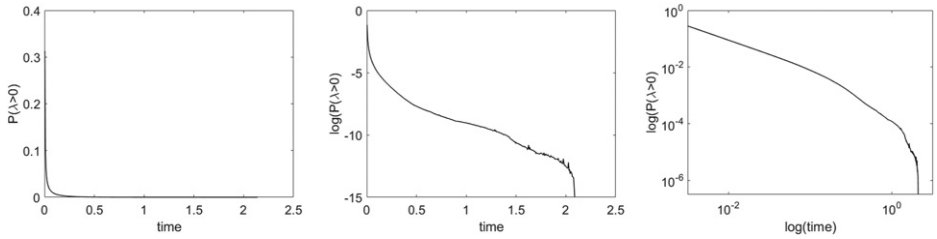

Figure 7. A plot of the relative frequency of positive exponents (as observed in figure 6) on (a) standard, (b) logarithmic and (c) log–log-scale.

typical points on the attractor (repeller),[7] one can pick almost any point (θ_0, x_0) and iterate it forwards (backwards) until—after some transition time—its trajectory follows the attractor so that with almost certainty, its further evolution reflects the behaviour of typical points.[8] Note that if we denote the right-hand side of (2) by $w(t, x)$, then evolving this equation backwards over an interval $[0, T]$ in time amounts to substituting $w(t, x)$ by $-w(T - t, x)$ and is therefore straightforward.

Hence, to numerically approximate, for example, the Lyapunov exponent of the attractor, we simply have to compute the pointwise Lyapunov exponent along a sufficiently long forward trajectory (after discarding its transient initial part), see (19) for the definition of the pointwise

[7] *Typical* with respect to natural ergodic measures on the respective equilibria, see section 2.

[8] In fact, a little more care is needed. When studying points on the attractor, one has to choose x_0 above the repeller to ensure that $\Xi^t(\theta_0, x_0)$ does not approach the equilibrium at $x = 0$. This is achieved by choosing x_0 above the autonomous equilibrium. Similarly, when iterating (θ_0, x_0) backwards to approximate the repeller, one has to ensure that x_0 is between both attractors. This is achieved by picking x_0 close to 0 but positive.

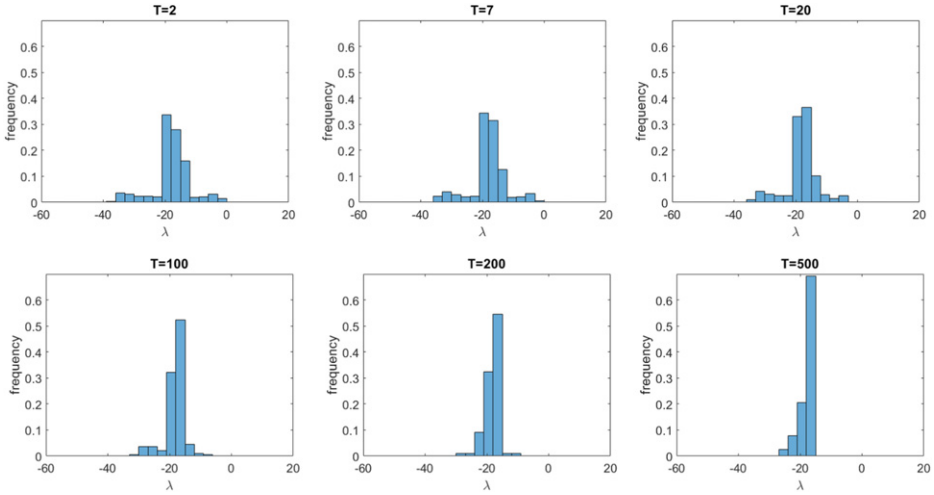

Figure 8. Distributions of the finite-time Lyapunov exponents in the randomly forced Allee model (2) with parameters $r = 80$, $K = 10$, $S = 0.1$, $\kappa = 6$ and $\beta = 13.978$ on different timescales, computed with sliding windows over a trajectory of length $t = 20\,000$.

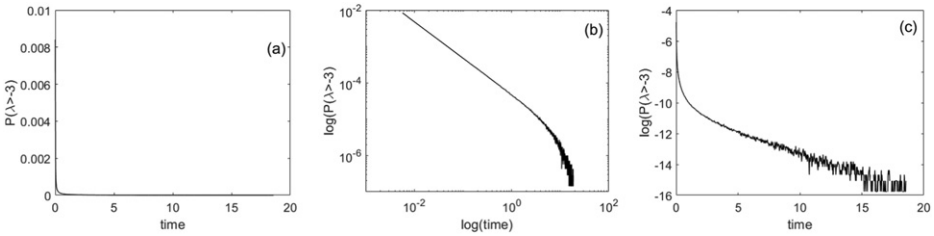

Figure 9. A plot of the relative frequency of positive exponents (as observed in figure 8) on (a) standard, (b) logarithmic and (c) log–log-scale.

Lyapunov exponent. By subdividing this long trajectory into multiple segments of a fixed time-length T, we can further compute multiple finite time Lyapunov exponents λ_T. We refer to such obtained values of λ_T as finite time Lyapunov exponents computed with a *sliding window* (of size T) over the respective trajectory. Note again that if the underlying trajectory is long enough, this collection of finite time Lyapunov exponents almost surely reflects the actual statistics of the finite time Lyapunov exponents on the attractor.

1.5.4. Further remarks. It should be pointed out that although finite-time Lyapunov exponents are—by definition—observable in finite time and may therefore in principle be accessible to experimental measurements, it is a difficult task to achieve and implement this for any real-life system. At the same time, a meaningful and practical definition of autocorrelation is difficult to provide for forced systems with moving random equilibria. Hence, the practical implementation of early-warning signals for critical transitions in forced systems remains a wide open problem, even in the simplest case of fold bifurcations.

On the theoretical side, an imminent problem that we tried to highlight by the above discussion is to give a precise mathematical meaning to terms like recovery rates, critical slowing

down as early warning signals and other notions that come up in the context of critical transitions. If theory and applications are supposed to go hand in hand, this will be an indispensable basis for further progress. The results and findings presented here should be understood as a contribution to that discussion.

1.5.5. Structure of the article. In section 2, we collect the required preliminary facts concerning the mathematical theory of non-autonomous dynamics and skew product systems, with a particular emphasis on invariant graphs and fold bifurcations in this setting. The application to the forced Allee model (2) is discussed in section 2.4. In section 2.5, we also introduce some discrete-time skew product systems, which may be thought of as simplified models for the time-one maps of the skew product flow induced by the forced Allee model. Section 3 is then devoted to the discussion of non-smooth fold bifurcation and also contains the proof of (a more general version of) theorem 2. The existence of the Lyapunov gap, stated in theorem 1, is proven in section 4, which also contains a result on the slope of the Lyapunov exponents at the bifurcation point (in the setting of the discrete-time model from section 2.5). Finite-time Lyapunov exponents are then defined and discussed in section 5, including the proof of (a more general version of) theorem 3.

2. Preliminaries

2.1. Skew product flows and invariant graphs

In order to treat continuous-time and discrete-time dynamics alongside, we let $\mathbb{T}$ be either equal to $\mathbb{R}$ (continuous-time) or $\mathbb{Z}$ (discrete-time). In both cases, a dynamical system is a pair (Y, Ξ) of a set Y and a $\mathbb{T}$-flow Ξ on Y, that is, a mapping

$$\Xi : \mathbb{T} \times Y \to Y, \quad (t, y) \mapsto \Xi^t(y) \tag{13}$$

which satisfies the flow properties

$$\Xi^0(y) = y \quad \text{and} \quad \Xi^{t+s}(y) = \Xi^t(\Xi^s(y)). \tag{14}$$

In the discrete-time case, this implies that $\Xi^t(y) = f^t(y)$, where $f : Y \to Y$ is the bijective map given by $f(y) = \Xi^1(y)$.

We always assume that Y is equipped with a σ-algebra $\mathcal{B}$. A probability measure μ on Y is called Ξ-invariant if $\mu \circ \Xi^t = \mu$ for all $t \in \mathbb{T}$. The set of all μ-invariant probability measures on $(Y, \mathcal{B})$ is denoted by $\mathcal{M}(\Xi)$. Given $\mu \in \mathcal{M}(\Xi)$, we call the quadruple $(Y, \mathcal{B}, \mu, \Xi)$ a *measure-preserving dynamical system (mpds)*. We refer to [Arn98] and references therein for details and background.

If Y is a metric space and Ξ is continuous on the product space $\mathbb{T} \times Y$, we call the pair (Y, Ξ) a *topological dynamical system (tds)*. In this case, we throughout assume $\mathcal{B}$ to be given by the Borel σ-algebra on Y.

Non-autonomous dynamics are modeled by skew product systems. Given a tds (Θ, ω) or an mpds $(\Theta, \mathcal{B}, \mu, \omega)$, a *skew product flow with base* Θ *and phase space* X is a flow on $Y = \Theta \times X$ of the form

$$\Xi : \mathbb{T} \times \Theta \times X \to \Theta \times X, \quad (t, \theta, x) \mapsto \Xi^t(\theta, x) = (\omega^t(\theta), \xi^t(\theta, x)). \tag{15}$$

Hence, if $\pi_\Theta : \Theta \times X$ is the canonical projection to Θ, then $\pi_\Theta \circ \Xi^t(\theta, x) = \omega^t(\theta)$. The maps $X \ni x \mapsto \xi^t(\theta, x) \in X$, with $t \in \mathbb{R}$ and $\theta \in \Theta$ fixed, are called *fibre maps*. If X is a metric space, we assume the fibre maps to be continuous without further mentioning. If X is a smooth manifold and all the fibre maps $\xi^t(\theta, \cdot)$ are r times differentiable, we call Ξ an ω-forced $\mathcal{C}^r$ flow. If $X = \mathbb{R}$ and the fibre maps are all monotonically increasing, we say Ξ is an *ω-forced monotone flow*.

As discussed already in the introduction, in the context of non-autonomous systems the notion of an equilibrium point has to be replaced by that of a random equilibrium, to which we will from now on refer to as an *invariant graph*, whose position depends on the forcing variable θ. We say a measurable function $\varphi : \Theta \to X$ is an *invariant graph* of the flow Ξ, if it satisfies the condition

$$\Xi^t_\theta(\varphi(\theta)) = \varphi(\omega^t(\theta)) \tag{16}$$

for all $\theta \in \Theta$ and $t \in \mathbb{T}$.[9] Here, we usually do not distinguish between invariant graphs that coincide almost everywhere with respect to the given reference measure in the base, which in the qpf case is just the Lebesgue measure. Hence, whenever we speak of invariant graphs, we implicitly mean equivalence classes of functions. This is very natural when Ξ is forced by an mpds, but may become a subtle issue as soon as Θ is a metric space and topological properties of invariant graphs come into play. For instance, by saying that an invariant graph is continuous, we mean that there exists a (uniquely determined) continuous representative of the respective equivalence class. It is worth mentioning that in the case of semi-continuous graphs, there may exist several different semi-continuous representatives in the same equivalence class—an issue that we will come back to in section 4 below. In the random case, we may not require that (16) is satisfied pointwise, but only almost surely. More precisely, if μ is an ω-invariant measure and (16) is satisfied μ-almost surely, then φ is called a $(\Xi,\ \mu)$-invariant graph.

It turns out that in the situation where base flow ω is ergodic, there is an intimate relation between invariant graphs and the invariant ergodic measures of the skew product system. Any $(\Xi,\ \mu)$-invariant graph φ clearly defines a Ξ-invariant measure μ_φ given by

$$\mu_\varphi(A) = \mu(\{\theta \in \Theta | (\theta, \varphi(\theta)) \in A\}). \tag{17}$$

A partial converse to this statement for ergodically forced monotone flows is provided by the following result, which essentially goes back to Furstenberg [Fur61] (see also [Arn98]) and highlights the significance of invariant graphs from an ergodic-theoretical viewpoint. Given $\mu \in \mathcal{M}(\omega)$, we denote by $\mathcal{M}_\mu(\Xi)$ the set of Ξ-invariant probability measures on $\Theta \times X$ which project to μ in the first coordinate.

Theorem 2.1 (See [Arn98, theorem 1.8.4] and [Fur61, theorem 4.1]). *Suppose Ξ is an ω-forced monotone flow, $\mu \in \mathcal{M}(\omega)$ is ergodic with respect to ω and $\nu \in \mathcal{M}_\mu(\Xi)$ is ergodic with respect to Ξ. Then there exists a $(\Xi,\ \mu)$-invariant graph φ such that $\nu = \mu_\varphi$.*

Hence, for monotone skew product flows with ergodic base flow there is a one-to-one correspondence between invariant ergodic measures and the invariant graphs of the system. Similar

[9] We use φ instead of x to denote invariant graphs from now on (unlike in the introduction) to stress the fact that these are functions.

to the autonomous case, the stability of an invariant graph φ can be characterised in terms of its *Lyapunov exponent*. The latter is given by

$$\lambda_\mu(\varphi) = \frac{1}{t}\int_\Theta \log \|\partial_x \xi^t(\theta, \varphi(\theta))\| \, \mathrm{d}\mu(\theta) = \int_\Theta \log \|\partial_x \xi^1(\theta, \varphi(\theta))\| \, \mathrm{d}\mu(\theta), \tag{18}$$

for any $t > 0$ where ∂_x denotes the derivative with respect to x and $\mu \in \mathcal{M}(\omega)$ is a given reference measure in the base. It is known that, under some mild assumptions, an invariant graph with negative Lyapunov exponent attracts a set of initial conditions of positive measure [Jäg03] (with respect to the product measure $\mu \times \mathrm{Leb}$ if $X = \mathbb{R}^d$, where Leb denotes the Lebesgue measure on $\mathbb{R}^d$). Hence, the graph φ is called an *attractor* in this case, and a *repeller* if $\lambda(\varphi) > 0$ [Fuh16a].

Observe that Birkhoff's ergodic theorem and the invariance of the graph φ imply that

$$\begin{aligned}\lambda_\mu(\varphi) &= \int_\Theta \log \|\partial_x \xi^1(\theta, \varphi(\theta))\| \, \mathrm{d}\mu(\theta) \\ &= \lim_{t\to\infty} 1/t \int_0^t \log \|\partial_x \xi^1(\omega^s(\theta), \varphi(\omega^s(\theta)))\| \, \mathrm{d}s \\ &= \lim_{t\to\infty} 1/t \int_0^t \log \|\partial_x \xi^1(\Xi^s(\theta, \varphi(\theta)))\| \, \mathrm{d}s = \lambda(\theta, \varphi(\theta))\end{aligned} \tag{19}$$

for μ-almost all $\theta \in \Theta$. In other words, the *pointwise Lyapunov exponent* $\lambda(\theta, x)$ of μ_φ-almost every point (θ, x) on φ coincides with the Lyapunov exponent of φ. As we will discuss in the final part of this article, the limit in the definition of $\lambda(\theta, \varphi(\theta))$ is in general not uniform. For that reason, the *time-T Lyapunov exponents*

$$\lambda_T(\theta, \varphi(\theta)) = 1/T \int_0^T \log \|\partial_x \xi^1(\omega^s(\theta)\, \xi^s(\theta\, \varphi(\theta)))\| \, \mathrm{d}s, \tag{20}$$

where $T > 0$, may carry relevant information different from that encoded in the (asymptotic) Lyapunov exponents.

An important notion in the context of forced systems is that of pinched sets and pinched invariant graphs [Gle02, Sta03, FJJK05, JS06, Jäg07]. *A priori*, the definition of *'pinching'* is independent of the dynamics. Suppose that Θ is a compact metric space, $X = [a, b] \subseteq \mathbb{R}$ and $\varphi^-, \varphi^+ : \Theta \to X$. Further, assume that φ^- is lower semi-continuous and φ^+ is upper semi-continuous and $\varphi^- \leqslant \varphi^+$. Then φ^- and φ^+ are called *pinched* if there exists a point $\theta \in \Theta$ with $\varphi^-(\theta) = \varphi^+(\theta)$. If we only have that for any $\varepsilon > 0$ there exists θ_ε with $|\varphi^+(\theta_\varepsilon) - \varphi^-(\theta_\varepsilon)| < \varepsilon$, then we call φ^+ and φ^- *weakly pinched*. In the case of random forcing, we will use the following measure-theoretic analogue. Suppose $(\Theta, \mathcal{B}, \mu)$ is a measure space, $X = [a, b] \subseteq \mathbb{R}$ and $\varphi^- \leqslant \varphi^+ : \Theta \to X$ are measurable. Then φ^- and φ^+ are called *measurably pinched* if the set $A_\delta := \{\theta \in \Theta | \varphi^+(\theta) - \varphi^-(\theta) < \delta\}$ has positive measure for all $\delta > 0$. Otherwise, we call φ^- and φ^+ μ-uniformly separated. For strictly ergodic (that is, minimal and uniquely ergodic) forcing processes, all three notions of pinching coincide, see [AJ02, lemma 3.5]. In this case, two pinched invariant graphs always coincide on a dense subset of Θ.

In order to define pinching for a set $M \subseteq \Theta \times X$, we let $M_\theta = \{x \in X | (\theta, x) \in M$ and define the *upper and lower bounding graphs of* M as $\varphi_M^+(\theta) = \sup M_\theta$ and $\varphi_M^-(\theta) = \inf M_\theta$. Then M is called *pinched/weakly pinched/measurably pinched* if this is true for its pair of bounding graphs (where in the topological setting M is supposed to be compact, which results in the respective semi-continuity of the graphs $\varphi_M^\pm$).

2.2. Fold bifurcation scenario

With the above notions, we can now formulate the bifurcation scenario—both in a deterministic and a random setting—which is taken from [AJ02] and will provide the general framework for our further studies. We start with the deterministic case. Given $A \subseteq \Theta \times X$ and $\theta \in \Theta$, we let $A_\theta = \{x \in X | (\theta, x) \in A\}$.

Theorem 2.2 ([AJ02, theorem 7.1]). *Let ω be a flow on a compact metric space Θ and suppose $(\Xi_\beta)_{\beta \in [0,1]}$ is a parameter family of ω-forced monotone $\mathcal{C}^2$ flows. Further assume that there exist continuous functions $\gamma^-, \gamma^+ : \Theta \to X$ with $\gamma^- < \gamma^+$ such that the following conditions hold for all $\beta \in [0,1]$, $\theta \in \Theta$ and all $t \geqslant 0$, where applicable.*

(*a*) *There exist two distinct continuous Ξ_0-invariant graphs and no Ξ_1-invariant graph in $\Gamma = \{(\theta, x) | \gamma^-(\theta) < x < \gamma^+(\theta)\}$;*
(*b*) $\xi_\beta^t(\theta, \gamma^\pm(\theta)) \leqslant \gamma^\pm(\omega^t(\theta))$;
(*c*) *The maps $(\beta, \theta, x) \mapsto \partial_x^i \xi_\beta^t(\theta, x)$ with $i = 0, 1, 2$ and $(\beta, \theta, x) \mapsto \partial_\beta \xi_\beta^t(\theta, x)$ are continuous;*
(*d*) $\partial_x \xi_\beta^t(\theta, x) > 0 \ \forall \ x \in \Gamma_\theta$;
(*e*) $\partial_\beta \xi_\beta^t(\theta, x) < 0 \ \forall \ x \in \Gamma_\theta$;
(*f*) $\partial_x^2 \xi_\beta^t(\theta, x) < 0 \ \forall \ x \in \Gamma_\theta$.

Then there exists a unique critical parameter $\beta_c \in [0,1]$ such that

- *If $\beta < \beta_c$, then there exist two continuous Ξ_β-invariant graphs $\varphi_\beta^- < \varphi_\beta^+$ in Γ. For any ω-invariant measure μ we have $\lambda_\mu(\varphi_\beta^-) > 0$ and $\lambda_\mu(\varphi_\beta^+) < 0$.*
- *If $\beta = \beta_c$, then either there exists exactly one continuous Ξ_β-invariant graph φ_β in Γ (smooth bifurcation), or there exists a pair of weakly pinched Ξ_β-invariant graphs $\varphi_\beta^- \leqslant \varphi_\beta^+$ in Γ with φ_β^- lower and φ_β^+ upper semi-continuous (non-smooth bifurcation). If μ is an ω-invariant measure, then in the first case $\lambda_\mu(\varphi_\beta) = 0$. In the second case $\varphi_\beta^-(\theta) = \varphi_\beta^+(\theta)$ μ-almost surely implies $\lambda_\mu(\varphi_\beta^\pm) = 0$, whereas $\varphi_\beta^-(\theta) < \varphi_\beta^+(\theta)$ μ-almost surely implies $\lambda_\mu(\varphi_\beta^-) > 0$ and $\lambda_\mu(\varphi_\beta^+) < 0$.*
- *If $\beta > \beta_c$, then no Ξ_β-invariant graphs exist in Γ.*

Remark 2.3. (a) Note that in [AJ02], the conditions of this theorem are stated in terms of the right side of the differential equation. However, [AJ02, section 7] provides a detailed discussion of how this translates into the above conditions on the flow, and these are the ones which are actually used in the proof. We come back to this issue in remark 2.4 below.

(b) A similar result for minimally forced flows induced by scalar differential equations is given in [NO07].

(c) The result in [AJ02] is stated for convex fibre maps. However, the above version for concave fibre maps is equivalent. For the discrete-time version, this is discussed in [AJ02, remark 6.2(c)].

(d) Likewise, the statement in [AJ02] is given for the closed region $\overline{\Gamma}$ instead of the open set Γ that we use here (for convenience later on), but the proof in [AJ02] can be adjusted with minor modifications.

(e) Non-continuous invariant graphs with negative Lyapunov exponents, as they appear in non-smooth fold bifurcation of qpf systems, are called *strange non-chaotic attractors* (SNA) [GOPY84, Kel96, Sta03, FKP06, NO07, AJ02].

Remark 2.4. Continuous-time skew product flows are typically defined via non-autonomous ODE's of the form

$$x'(t) = V(\omega^t(\theta), x). \tag{21}$$

In fact, (21) *a priori* only yields a *local* flow where trajectories may diverge and hence not be defined for all times $t \in \mathbb{R}$. As we will only deal with bounded solutions (see also lemma 3.6), this issue is not of further importance. We refer the interested reader to [Fuh16b] for more details.

Now, in order to apply theorem 2.2 to flows defined by equations of the form (21), it is crucial that the validity of the assumptions can be read off directly from the differential equations. Fortunately, there is a rather immediate translation between the properties of parameter families of non-autonomous vector fields V_β and the relevant properties of the resulting skew product flow.

First, the curves $\gamma^\pm$ can usually be chosen constant, in which case (a) may be obvious or be checked by hand for the respective models and (b) follows from $V_\beta(\theta, \gamma^\pm(\theta)) < 0$ for all $\theta \in \Theta$. Secondly, by standard results on the regularity of solutions of an ODE with respect to parameters, it suffices to assume that for each $\theta \in \Theta$ the mapping $[0,1] \times \mathbb{R} \times \mathbb{R} \ni (\beta, t, x) \mapsto V_\beta(\omega^t(\theta), x)$ is continuous, $\mathcal{C}^1$ with respect to β, and $\mathcal{C}^2$ with respect to x in order to ensure that Ξ_β is indeed $\mathcal{C}^2$ and continuously differentiable with respect to β. Hence, the condition (c) will hold as well. The monotonicity in (d) follows immediately from the uniqueness of the solutions to (21). The monotonicity condition (e) always holds if $\beta \mapsto V_\beta(\omega^t(\theta), x)$ is monotonically decreasing. Finally, the concavity of the fibre maps required in (f) is a consequence of the concavity of V_β in the considered region. We refer to [AJ02, Fuh16b], as well as to the discussion of the application to the forced Allee model in section 2.4, for further details.

The following statement is a measure-theoretic analogue of theorem 2.2. While this result is not explicitly stated in [AJ02], the article contains a discrete-time analogue and the translation to the continuous-time setting is both straightforward and also discussed in detail for the deterministic case in [AJ02, section 7].

Theorem 2.5 (Compare [AJ02, theorem 4.1]). *Let $(\Theta, \mathcal{B}, \mu, \omega)$ be a measure preserving dynamical system and suppose $(\Xi_\beta)_{\beta\in[0,1]}$ is a parameter family of ω-forced monotone $\mathcal{C}^2$ flows. Further assume that there exist measurable functions $\gamma^-, \gamma^+ : \Theta \to X$ with $\gamma^- < \gamma^+$ such that the following conditions hold for all $\beta \in [0,1]$, μ-almost all $\theta \in \Theta$ and all positive $t \in \mathbb{T}$, where applicable.*

- (*a*) *There exist two μ-uniformly separated (Ξ_0, μ)-invariant graphs but no (Ξ_1, μ)-invariant graph in Γ;*
- (*b*) $\xi^t_\beta(\theta, \gamma^\pm(\theta)) \leqslant \gamma^\pm(\omega^t(\theta))$*;*
- (*c*) *The maps $(\beta, t, x) \mapsto \xi^t_\beta(\theta, x)$ and $(\beta, t, x) \mapsto \partial_x \xi^t_\beta(\theta, x)$ are continuous;*
- (*d*) $\partial_x \xi^t_{\beta,\theta}(x) > 0 \ \forall\ x \in \Gamma_\theta$*;*

(*e*) *For some* $t > 0$ *there exist constants* $C < c_1 \leqslant 0$ *such that* $C \leqslant \partial_\beta \xi^t_\beta(\theta, x) \leqslant c_1 \ \forall\ x \in \Gamma_\theta$*;*
(*f*) $\partial^2_x \xi^t_\beta(\theta, x) < 0 \ \forall\ x \in \Gamma_\theta$*;*
(*g*) *The function* $\eta(\theta) = \sup\left\{|\log \partial_x \xi^t_\beta(\theta, x)| \,\middle|\, x \in \Gamma_\theta, \beta \in [0,1]\right\}$ *is integrable with respect to* μ*.*

Then there exists a unique critical parameter $\beta_\mu \in [0,1]$ *such that*

- *If* $\beta < \beta_\mu$*, then there exist exactly two* $(\Xi_\beta,\ \mu)$*-invariant graphs* $\varphi^-_\beta < \varphi^+_\beta$ *in* Γ *which are* μ*-uniformly separated and satisfy* $\lambda(\varphi^-_\beta) > 0$ *and* $\lambda(\varphi^+_\beta) < 0$*.*
- *If* $\beta = \beta_\mu$*, then either there exists exactly one* $(\Xi_\beta,\ \mu)$*-invariant graph* φ_β *in* Γ*, or there exist two measurably pinched invariant graphs* $\varphi^-_\beta \leqslant \varphi^+_\beta$ *in* Γ*. In the first case,* $\lambda_\mu(\varphi_\beta) = 0$*; in the second case,* $\lambda_\mu(\varphi^-_\beta) > 0$ *and* $\lambda_\mu(\varphi^+_\beta) < 0$*.*
- *If* $\beta > \beta_\mu$*, then no* f_β*-invariant graphs exist in* Γ*.*

In analogy to the deterministic setting, we again speak of a smooth bifurcation if there exists a unique neutral invariant graph at the bifurcation point, and of a non-smooth bifurcation if there exists an attractor-repeller pair (a pair of pinched invariant graphs with negative and positive Lyapunov exponent, respectively).

Remark 2.4 concerning how to ensure the conditions are met by the flow induced by a non-autonomous vector field equally apply in the random setting. Note that continuity with respect to θ is not required in this case.

2.3. Forcing processes

For later use, we introduce forcing processes both in discrete and continuous time. Quasiperiodic motion in discrete time is given by a rotation $\omega : \mathbb{T}^d \to \mathbb{T}^d,\ \theta \mapsto \theta + \rho \mod 1$ which is *irrational*, in the sense that its rotation vector $\rho = (\rho_1, \ldots, \rho_d)$ has incommensurate entries.[10] In this case, the transformation ω is minimal and uniquely ergodic, with the Lebesgue measure on $\mathbb{T}^d$ as the unique invariant probability measure. The continuous time analogue is an irrational Kronecker flow $\omega : \mathbb{R} \times \mathbb{T}^d \to \mathbb{T}^d,\ \omega^t(\theta) = \theta + t\rho$, where ρ (or some scalar multiple thereof) is again incommensurate.

In order to model random forcing in discrete time, we will simply use Bernoulli processes as examples. Hence, we let $\Sigma = \{0,1\}^{\mathbb{Z}}$ and equip this space with the Bernoulli measure μ with probabilities 1/2 for the symbols 0 and 1. Actually, we could likewise set Σ to be $[0,1]^{\mathbb{Z}}$ and μ to be the infinite product $\mathrm{Leb}^{\mathbb{Z}}_{[0,1]}$ of the Lebesgue measure on [0, 1], or even replace $\mathrm{Leb}_{[0,1]}$ by any measure λ on [0, 1] whose topological support includes 0 and 1. In any case, the dynamics on Σ are given by the shift map $\sigma : \Sigma \ni (\theta_n)_{n\in\mathbb{Z}} \mapsto (\theta_{n+1})_{n\in\mathbb{Z}}$ which is ergodic with respect to each such measure.

A slight complication occurs in the case of continuous-time random forcing. As mentioned in the introduction, we would like to use $\sin(W_t)$ as a forcing term in (2). Hence, it is natural to consider the Wiener space, that is, the space of continuous real-valued functions $\mathcal{C}(\mathbb{R}, \mathbb{R})$ equipped with the Borel σ-algebra generated by uniform topology and the classical Wiener measure $\mathbb{P}$. However, in order to obtain a skew product flow we need a measure-preserving transformation on our probability space. If $\theta \in \mathcal{C}(\mathbb{R}, \mathbb{R})$ is a path of a Brownian motion, the standard measure-preserving shift on the Wiener space is given by $\omega^t(\theta)(s) = \theta(s + t) - \theta(t)$. The problem that occurs is the fact that if we now want to define a forcing term f on $\mathcal{C}(\mathbb{R}, \mathbb{R})$ by evaluating the sinus at $\theta(0)$, that is, $f(\theta) = \sin(2\pi\theta(0))$, then $f(\omega^t(\theta)) = 0$ for all $t \in \mathbb{R}$ (the standard Brownian motion starts in zero, and the classical shift respects this property). We

[10] Here $\rho_1, \ldots, \rho_d$ are called *incommensurate* if $n_0 + \sum_{j=1}^d n_j\rho_j = 0$ implies $n_0 = n_1 = \ldots = n_d = 0$.

therefore use a slightly modified version of this process to model bounded random forcing for our purposes. To that end, we let $p : \mathcal{C}(\mathbb{R}, \mathbb{R}) \to \mathcal{C}(\mathbb{R}, \mathbb{T}^1) = \Theta$ be the projection of real-valued to circle-valued functions (induced by the canonical projection $\pi : \mathbb{R} \to \mathbb{T}^1$) and let $\mathbb{P}_0 = p_*\mathbb{P}$ be the push-forward of $\mathbb{P}$. Further, we let $S : \mathbb{T}^1 \times \Theta \to \Theta,\ (x, \theta) \mapsto \theta + x$ and equip Θ with the measure $\nu = S_*(\mathrm{Leb}_{\mathbb{T}^1} \times \mathbb{P}_0)$. By definition, ν has equidistributed marginals and can therefore be seen to be invariant under the shift $\omega : \mathbb{R} \times \Theta \to \Theta$ defined by $\omega^t(\theta)(s) = \theta(t + s)$. This construction will allow us to define a forcing term simply by evaluating the sinus (viewed as a function on $\mathbb{T}^1$) at $\theta(0)$.

2.4. Application to the forced Allee model

In order to apply the above theorems 2.2 and 2.5 to the forced Allee model (2) with forcing terms (3) and (4), respectively, we first have to bring this equation into a form that fits into the mathematical setting described above. Note that the vector field V in (21) does not depend on a real time-variable t, but on a variable θ that belongs to the driving space Θ. The time-dependence then enters the equation via the forcing flow ω. This means that we need to slightly modify our initial equation (2) by assuming that the forcing function F in (2) is not defined on $\mathbb{R}$, but is given as a map $F : \Theta \to [0, 1]$ on one of the driving spaces discussed in the previous section. The time-dependence is then given by replacing $F(t)$ in (2) with $F(\omega^t(\theta))$, where ω is the forcing flow on Θ and $\theta \in \Theta$ is an arbitrary starting point. Hence, we arrive at the following modified version of (2).

$$x'(t) = \frac{r}{K^2} \cdot x(t) \cdot (K - x(t)) \cdot (x(t) - S) - (\beta + \kappa \cdot F(\omega^t(\theta))) \cdot x \ =: \ V_{\kappa,\beta}(\theta, x) \tag{22}$$

In the case of quasiperiodic forcing, we then let $\Theta = \mathbb{T}^d$ and

$$F : \mathbb{T}^d \to [0, 1], \qquad \theta \mapsto \prod_{i=1}^{d} \left(\frac{1 + \sin(2\pi(\theta_i))}{2} \right)^q. \tag{23}$$

Further, we let ω denote the Kronecker flow on T^d (with irrational translation vector ρ) introduced in the last section. Note that the differential equation given by (2) and (3) and the one given by (22) and (23) are identical.

Similarly, in the case of random forcing we let $\Theta = \mathcal{C}(\mathbb{R}, \mathbb{T}^1)$ equal the projected Wiener space introduced in the last section and let

$$F : \Theta \to [0, 1], \qquad \theta \mapsto \frac{1 + \sin(2\pi\theta(0))}{2} \tag{24}$$

and choose ω to be the shift on Θ introduced in the previous section. Then again the differential equations defined by (2) and (24) are the same.

We now want to verify that the skew product flow induced by (22) satisfies the assumptions of theorem 2.2 (for the quasiperiodic forcing term (23)) or theorem 2.5 (for the random forcing term (24). More precisely, we need to specify the admissible parameter ranges stated in remark 1.3 in the introduction and show that the respective conditions are met for all admissible parameters. As pointed out in remark 2.4, conditions (c)–(e) in theorems 2.2 and 2.5 follow directly from the specific form of the scalar field $V_{\beta,\kappa}$. Moreover, condition (g) in theorem 2.5 holds as well, since all the involved functions are bounded (and therefore, in particular, integrable). However, it remains to specify a suitable parameter range and appropriate functions $\gamma^{\pm}$ so that (a), (b) and (f) hold.

It is easy to check that the fold bifurcation of the unforced equation (1) takes place at

$$\beta = b(r,K,S) \;:=\; \frac{r}{K^2}\cdot\left(\frac{K-S}{2}\right)^2. \tag{25}$$

Moreover, the neutral equilibrium point at the bifurcation is $x_0 = \frac{K+S}{2}$. If $\kappa < b(r,K,S)$ and $\beta \leqslant b(r,K,S) - \kappa$, then we have that $V_{\kappa,\beta}(\theta,x_0) > 0$ for all $\theta \in \Theta$ and both forcing terms (3) and (4) (note here that $F \leqslant 1$). At the same time, given $\beta < b(r,K,S)$, the unforced Allee model (1) has equilibrium points $x = 0$ and

$$x^{\pm}_{\beta} = \frac{K+S}{2} \;\pm \frac{1}{2}\sqrt{(K-S)^2 - \frac{4\beta K^2}{r}} = \frac{K+S}{2} \;\pm \frac{K-S}{2}\cdot\sqrt{1-\bar{\beta}},$$

where

$$\bar{\beta} = \frac{4\beta K^2}{r(K-S)^2}.$$

As the forcing is always downwards (recall that the forcing term is $-\kappa F$ with $\kappa \geqslant 0$ and $F \geqslant 0$), this implies in particular that $V_{\kappa,\beta}(\theta, x^{\pm}_{\beta_0}) < 0$ for all $\theta \in \Theta$, $\kappa > 0$ and $\beta \geqslant \beta_0$. Hence, we obtain a forward invariant region $\Theta \times [x_0, x^{+}_{\beta_0}]$ and a backward invariant region $\Theta \times [x^{-}_{\beta_0}, x_0]$, where β_0 will be specified below. Using the concavity of $V_{\kappa,\beta}$ in x, equally shown below, this implies the existence of two invariant graphs in $[\gamma^-,\gamma^+] = [x^{-}_{\beta_0}, x^{+}_{\beta_0}]$. Similarly, if $\beta > b(r,K,S)$, then the bifurcation has already taken place and there will not be any invariant graph above the equilibrium at 0. Hence, conditions (a) and (b) are satisfied.

It remains to ensure the concavity of $V_{\kappa,\beta}(\theta,\cdot)$ in the considered region $\Theta \times (\gamma^-,\gamma^+)$, where $\gamma^{\pm}$ still need to be specified. The second derivative of $V_{\kappa,\beta}$ with respect to x is given by

$$\partial_x^2 V_{\kappa,\beta}(\theta,x) = \frac{r}{K^2}\cdot(-6x + 2(K+S)),$$

and is thus independent of β and κ. We have

$$\partial_x^2 V_{\kappa,\beta}(\theta,x) < 0 \quad\Leftrightarrow\quad x \;>\; \frac{K+S}{3}.$$

Hence, we simply need to choose β_0 such that $x^{-}_{\beta_0} \geqslant \frac{K+S}{3}$. By the above, this means that we require

$$x^{-}_{\beta} = \frac{K+S}{2} \;-\frac{K-S}{2}\cdot\sqrt{1-\bar{\beta}} \;\geqslant\; \frac{K+S}{3},$$

which is equivalent to

$$\bar{\beta} \;\geqslant\; 1 - \gamma(K,S),$$

where $\gamma(K,S) = \frac{1}{9}\left(\frac{K+S}{K-S}\right)^2$, and hence to

$$\beta \;\geqslant\; b(r,K,S)\cdot(1-\gamma(K,S)).$$

This means that if $\kappa > 0$ satisfies

$$\kappa \;<\; b(r,K,S)\cdot\gamma(K,S)$$

and we let

$$J(r,K,S) = [b(r,K,S)\cdot(1-\gamma(K,S)), b(r,K,S)+1],$$

then the parameter family of flows Ξ_β induced by the vector fields $(V_{\kappa,\beta})_{\beta\in J(r,K,S)}$ satisfies all the assertions of theorem 2.2 (modulo rescaling the parameter interval $J(r,K,S)$) and therefore undergoes a non-autonomous fold bifurcation.

2.5. A simplified discrete-time model

As mentioned in the introduction, in order to reduce the technical effort of our investigation, some of our rigorous results deal with discrete time systems. Of course, in principle, it would be most natural to consider the Poincaré sections of the continuous time models associated to (2). However, to prove that those actually satisfy the properties we need in our analysis turns out to be a surprisingly tough problem in itself, which, furthermore, does not appear to provide any insights into the behaviour of the (finite time) Lyapunov exponents.[11] Instead, we consider explicit paradigm examples which allow us to concentrate on those aspects of the dynamics which this work focuses on.

Specifically, we consider the parameter families of skew product maps

$$f_\beta : \Theta\times\mathbb{R}\to\Theta\times\mathbb{R}, \qquad (\theta,x)\mapsto(\omega(\theta), \arctan(\alpha x)-\kappa\cdot F(\theta)-\beta) \tag{26}$$

with real parameters $\alpha > \pi/2$, $\beta\in[0,1]$ and $\kappa\in(0,\tilde\beta_c)$, where $\tilde\beta_c = \arctan(\sqrt{\alpha-1}) - \sqrt{\alpha-1}/\alpha$ is the critical parameter at which the fold bifurcation of the autonomous family $x\mapsto\arctan(\alpha x)-\beta$ occurs. It is worth mentioning that—besides some important features of the above models—the precise choice of the fibre maps in (26) is more for the sake of concreteness than of actual mathematical relevance, see [Fuh16a].

The forcing processes we consider are either defined on $\Theta=\mathbb{T}^d$ and given by a rotation $\omega:\theta\mapsto\theta+\rho$ with rotation vector $\rho\in\mathbb{T}^d$ (quasiperiodic forcing) or on $\Theta=\Sigma$, where $\Sigma=\{0,1\}^{\mathbb{Z}}$ and ω is given by the shift σ on Σ (random forcing), all as in section 2.3 above. For the forcing function F, we use

$$F(\theta) = \frac{\sin(2\pi\theta)+1}{2} \tag{27}$$

in the qpf case and

$$F(\theta) = \theta_0 \tag{28}$$

in the random case. As figure 10 (to be compared to figure 3) and figures 12–14 (to be compared to figures 5–7) indicate, the phenomena we discussed for the forced Allee model remain observable when we go over to the above kind of systems.

The behaviour of the attractors and repellers during smooth and non-smooth bifurcations in the qpf case are shown in figure 11. This figure also illustrates some key features of non-smooth bifurcations in qpf systems and allows us to give a heuristic description of the mechanism that causes the non-smoothness. The rigorous description of this mechanism is the basis for the mathematical analysis of non-smooth bifurcations in [Jäg09, Fuh16a]. As can be seen in figures 11(d)–(f), when the attracting and repelling graphs approach each other in a non-smooth way, they develop a sequence of 'peaks'. These appear in an ordered way, and the

[11] The interested reader may take a look at [Fuh16b] for an example of the analysis of a very simplified non-autonomous continuous time system through an associated Poincaré map.

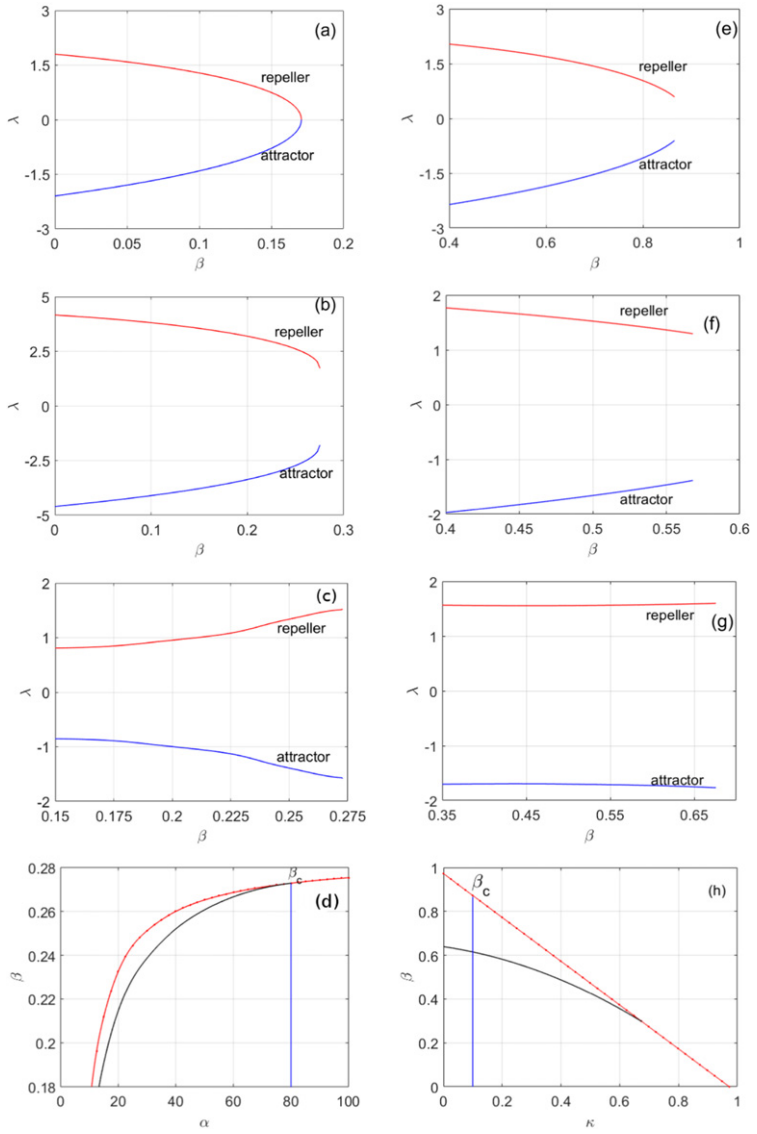

Figure 10. Lyapunov exponents during saddle-node bifurcations in the family (26) with forcing terms (27) (quasiperiodic) and (28) (random). The plots are analogous to those shown in figure 3 for the forced Allee model. Just as for that model, the behaviour of the Lyapunov exponents depends fundamentally on the precise form of the considered parameter changes. (a) Smooth bifurcation in the qpf case, with parameters $\alpha = 10$ and $\kappa = 1$. The bifurcation occurs at $\beta_c = 0.341\,502$. (b) A non-smooth bifurcation in the same model, with parameters $\alpha = 100$ and $\kappa = 1$. The bifurcation occurs at $\beta_c = 0.550\,7468$. (c) Non-smooth bifurcation with simultaneous variation of parameters α and β along the black curve in (d). (e) and (f) Lyapunov exponents in the rdf case, with parameters $\alpha = 10$ and $\kappa = 0.1$ and bifurcation parameter $\beta = 0.866$ in (e) and $\alpha = 10$ and $\kappa = 0.4$ and bifurcation parameter $\beta = 0.566$ in (f). In (g), the parameters κ and β are varied again at the same time along the black parameter curve shown in (h).

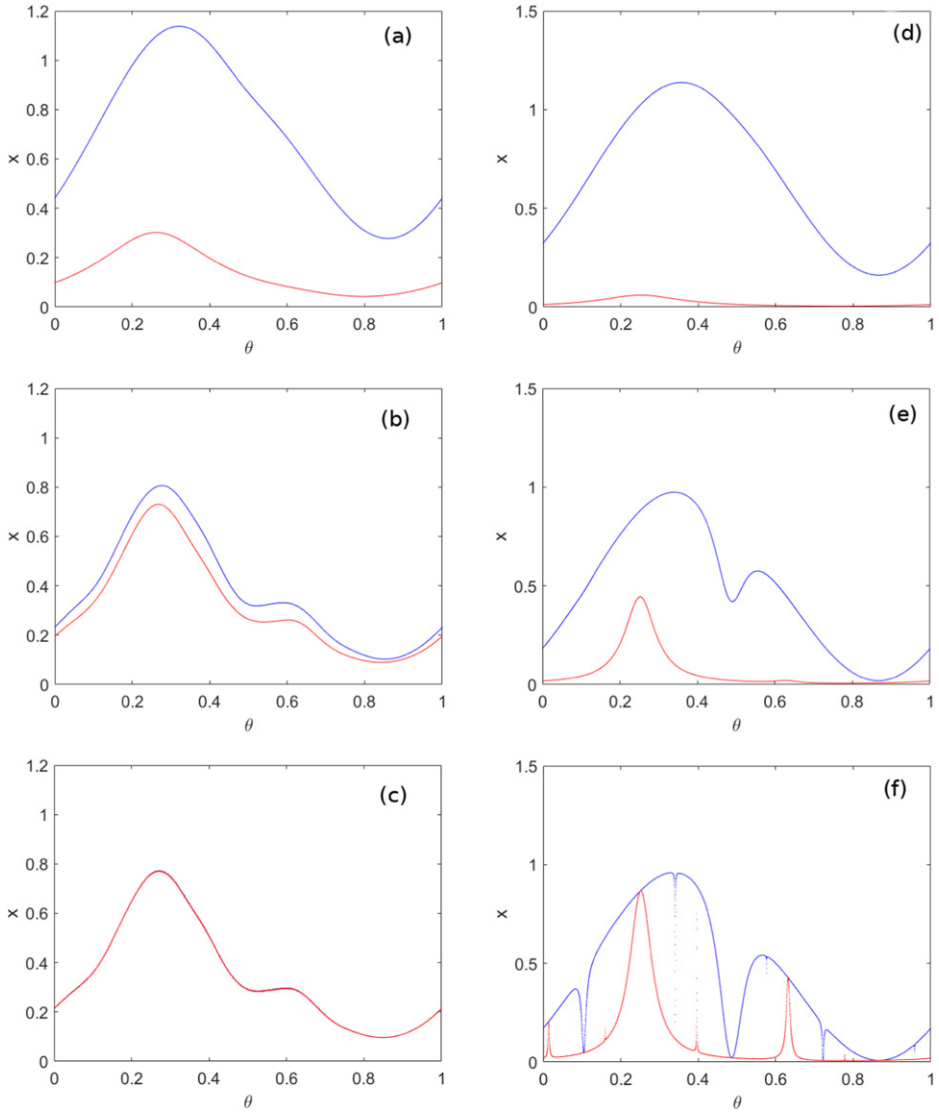

Figure 11. (a)–(c) Smooth saddle-node bifurcation in (26) with quasiperiodic forcing (27). Parameter values are $\alpha = 10$, $\kappa = 1$, $\rho = \omega$ (golden mean) and (a) $\beta = 0.1708$ (b) $\beta = 0.34$ and (c) $\beta = 0.341\,502$. (d)–(f) Non-smooth saddle-node bifurcation bifurcation in in (26) with quasiperiodic forcing (27). Parameter values are $\alpha = 100$, $\kappa = 1$, $\rho = \omega$ and (a) $\beta = 0.4$ (b) $\beta = 0.54$ and (c) $\beta = 0.550\,7486$.

next peak is always the image of the previous one and is generated as soon as the latter reaches into the region with large derivatives which is centred around the zero-line $\mathbb{T}^1 \times \{0\}$. The first peak is located around the minimum of the blue curve in (d). The second peak emerges in (e) and is fully developed in (f), where a number of further peaks can be seen as well. Thereby, the movement of each peak is amplified by the large derivatives close to zero (of magnitude α, see (26)). For this reason, as β is increased, the speed by which the peaks move as β is varied increases exponentially with the order of the peak, whereas its width decreases exponentially

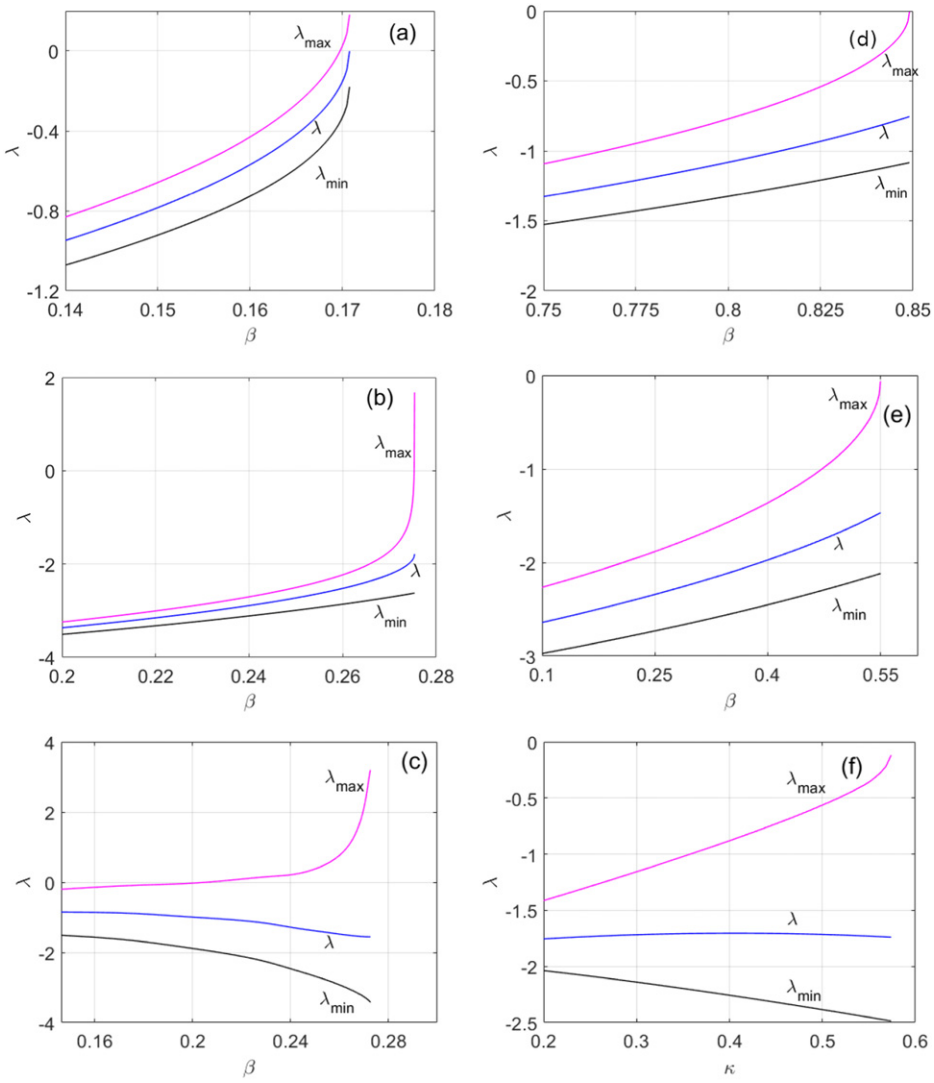

Figure 12. Minimal and maximal finite-time Lyapunov exponents (with the asymptotic one plotted in the middle) for the parameter families used in figure 10 (in the same order). The time is $n = 5$ in all cases. Observe that just as in the forced Allee model (see figure 5), an approaching bifurcation is anticipated by maximal finite time Lyapunov exponents above or close to 0.

(since each peak is stretched vertically due to the expansion around 0). In the limit, the two curves touch each other with the tips of the peaks. Note that only a finite number of peaks can be observed at the bifurcation point in (f), since these quickly become too thin to be visible in numerical simulations. However, it is known that the region between the two graphs in (f) is actually filled densely by further peaks [GJ13, FGJ18]. We refer to the introduction of [Jäg09] for a more detailed discussion.

The range of the finite time Lyapunov exponents for the same parameter families as in figure 10 is shown in figure 12.

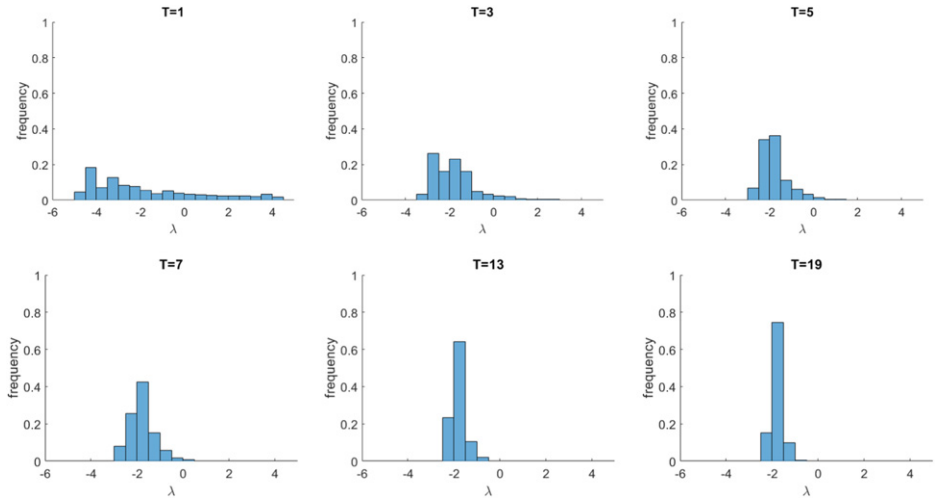

Figure 13. Distributions of the finite-time Lyapunov exponents in the qpf discrete-time system (26) with parameters $\alpha = 100$, $\kappa = 1$ and ρ the golden mean. Observe again the qualitative similarity to the distribution of finite time Lyapunov exponents in the forced Allee model (figure 6).

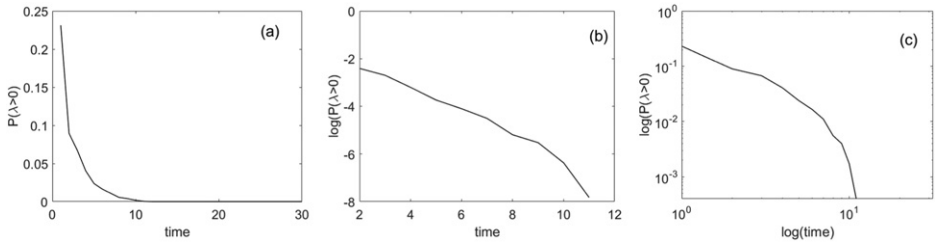

Figure 14. A plot of the relative frequency of positive exponents (as observed in figure 13) on a (a) standard, (b) logarithmic and (c) log–log-scale.

Finally, the distribution of finite-time Lyapunov exponents (on different time-scales) is plotted in figure 13, and the corresponding relative frequencies as a function of time in figure 14. In both cases, we restrict to the qpf case.

3. Abundance of nonsmooth fold bifurcations

The results discussed in the previous section provide a general setting for non-autonomous saddle-node bifurcations. We shall now take a closer look at non-smooth bifurcations and discuss their widespread occurrence in forced systems.

3.1. Quasiperiodic forcing

In the case of quasiperiodic forcing, the latter is well-established by a number of rigorous results both in the discrete- and continuous-time case. In order to state these, we need to introduce some arithmetic properties of the rotation numbers or vectors in the base, which play a

crucial role. Given $\tau, \kappa > 0$, we say $\rho \in \mathbb{T}^d$ is *Diophantine (of type* (τ, κ)*)* if

$$\forall\, k \in \mathbb{Z}^d \backslash \{0\} : \inf_{p \in \mathbb{Z}} \left| p + \sum_{i=1}^{d} \rho_i k_i \right| \geqslant \tau |k|^{-\kappa}.$$

We note that the set of rotation vectors that satisfy a Diophantine condition of type (τ, κ) for some $\tau > 0$ (with κ fixed) is of full Lebesgue measure for all $\kappa > \frac{d+1}{d}$.

Let us start by considering the discrete-time case. Generalising example (26), consider discrete-time flows given by qpf monotone interval maps of the form

$$f : \mathbb{T}^d \times \mathbb{R} \to \mathbb{T}^d \times \mathbb{R}, \qquad (\theta, x) \mapsto (\omega(\theta), f_\theta(x)), \tag{29}$$

where $\omega : \mathbb{T}^d \to \mathbb{T}^d, \theta \mapsto \theta + \rho$ is again an irrational rotation with rotation vector ρ and $f_\theta(\cdot)$ is $\mathcal{C}^2$ and strictly increasing on X. For a given rotation vector $\rho \in \mathbb{T}^d$, we further consider the space of one-parameter families

$$\mathcal{F}_\rho = \left\{ (f_\beta)_{\beta \in [0,1]} : f_\beta \text{ is of form (29) and } (\beta, \theta, x) \mapsto f_{\beta,\theta}(x) \text{ is } \mathcal{C}^2 \right\} \tag{30}$$

equipped with the metric

$$d((f_\beta)_{\beta \in [0,1]}, (g_\beta)_{\beta \in [0,1]}) = \sup_{\beta \in [0,1]} (\|f_\beta - g_\beta\|_2 + \|\partial_\beta f_\beta - \partial_\beta g_\beta\|_0), \tag{31}$$

where $\|.\|_k$ denotes the $\mathcal{C}^k$-norm on the space $\mathcal{D}^k(\mathbb{T}^d \times X)$ of k times differentiable self-maps of $\mathbb{T}^d \times X$. Note that all maps f_β in parameter families from $\mathcal{F}_\rho$ have the same base flow $\omega : \theta \mapsto \theta + \rho$ on $\mathbb{T}^d$.

The following result has been established in [Fuh16a], with precursors in [Bje05, Jäg09].

Theorem 3.1 ([Fuh16a]). *Suppose that $\rho \in \mathbb{T}^d$ is Diophantine. Then there exists a non-empty open set $\mathcal{U} \subseteq \mathcal{F}_\rho$ such that each $(f_\beta)_{\beta \in [0,1]} \in \mathcal{U}$ satisfies the assertions of theorem 2.2 and undergoes a non-smooth saddle-node bifurcation.*

This confirms that the set of parameter families with a non-smooth saddle-node bifurcation is large in a certain sense, and that the phenomenon can occur in a robust way (both corresponding to the openness of the set $\mathcal{U}$). Thereby, it is important to note that in [Fuh16a] the set $\mathcal{U}$ in this result is characterised by explicit $\mathcal{C}^2$-estimates involving derivatives with respect to all three variables β, θ and x. This makes it possible to check whether it contains a given parameter family and therefore provides explicit examples of non-smooth saddle-node bifurcations.

Corollary 3.1.1 ([Fuh16a]). *If ρ is Diophantine and α is sufficiently large, then the parameter family $(f_\beta)_{\beta \in [0,1]}$ defined in (26) belongs to the set $\mathcal{U}$ and hence undergoes a non-smooth saddle-node bifurcation.*

Continuous-time analogues of these results have been established in [Fuh16b]. In this case, one considers non-autonomous vector fields, given by differentiable functions of the form

$$V : \mathbb{T}^d \times \mathbb{R} \to \mathbb{R}, \tag{32}$$

which induce qpf flows via the corresponding differential equation

$$x'(t) = V(\omega_t(\theta_0), x(t)), \tag{33}$$

where $\omega : \mathbb{R} \times \mathbb{T}^d \to \mathbb{T}^d,\ (t, \theta) \mapsto \theta + t\rho$ is an irrational Kronecker flow with rotation vector $\rho \in \mathbb{T}^d$, as described above. We let

$$\mathcal{V} = \left\{(V_\beta)_{\beta\in[0,1]} | V \text{ is of the form (32) and } (\beta, \theta, x) \mapsto V_\beta(\theta, x) \text{ is } \mathcal{C}^2\right\} \tag{34}$$

and equip $\mathcal{V}$ with the metric

$$d((V_\beta)_{\beta\in[0,1]}, (W_\beta)_{\beta\in[0,1]}) = \sup_{\beta\in[0,1]} (\|V_\beta - W_\beta\|_2 + \|\partial_\beta V_\beta - \partial_\beta W_\beta\|_0).$$

Theorem 3.2 ([Fuh16b]). *For any Diophantine $\rho \in \mathbb{T}^d$, there exists an open set $\mathcal{U}_\rho \subseteq \mathcal{V}$ such that for any $(V_\beta)_{\beta\in[0,1]} \in \mathcal{V}$ the flow induced by (32) satisfies the assertions of theorem 2.2 and undergoes a non-smooth fold bifurcation.*

Again, the explicit characterisation of the set $\mathcal{U}_\rho$ given in [Fuh16b] makes it in principle possible to check for non-smooth bifurcations in specific examples. However, this is considerably more technical than in the discrete-time case. Moreover, the application to the forced Allee model (2) with quasiperiodic forcing (3) would require a number of highly non-trivial and technical modifications. Therefore, we refrain from going into more details here and just point out that figures 2(b) and 4(e)–(h) provide substantial numerical evidence for the occurrence of non-smooth fold bifurcations in this case.

3.2. Random forcing

In contrast to the quasiperiodic case, the influence of bounded random noise on saddle-node bifurcations has not been studied systematically so far. Our aim for the remainder of this section is to establish the occurrence of non-smooth bifurcations in a broad class of rdf monotone flows and maps. To that end, we introduce the notion of an autonomous reference system. Let $\gamma^- < \gamma^+ \in \mathbb{R}$ and suppose $(g_\beta)_{\beta\in[0,1]}$ is a one-parameter family of differentiable flows $g_\beta : \mathbb{T} \times \mathbb{R} \to \mathbb{R}$ with the following properties (which are supposed to hold for all $\beta \in [0, 1], t \in \mathbb{T}$ and $x \in \mathbb{R}$, where applicable).

(g1) g_0 has two fixed points in the interval $[\gamma^-, \gamma^+]$, whereas g_1 has none;
(g2) $g^t_\beta(\gamma^\pm) \leqslant \gamma^\pm$;
(g3) $\partial_x g^t_\beta(x) > 0$;
(g4) The mapping $(\beta, t, x) \mapsto g^t_\beta(x)$ is continuous;
(g5) The mapping $\beta \mapsto g^t_\beta(x)$ is differentiable and $\partial_\beta g^t_\beta(x) < 0$;
(g6) $\partial^2_x g^t_\beta(x) < 0$ for all $x \in [\gamma^-, \gamma^+]$ *(concavity).*

We call such a family $(g_\beta)_{\beta\in[0,1]}$ an *(autonomous) reference family*.

Remark 3.3. (a) Properties (g1)–(g6) imply that the family $(g_\beta)_{\beta\in[0,1]}$ undergoes a fold bifurcation in the interval $[\gamma^-, \gamma^+]$: due to the concavity in (g6), g_β can have at most two fixed points in this region, with the upper one attracting and the lower one repelling. By (g1), the map g_0 has two such fixed points. Due to the monotone dependence on the parameter assumed in (g5), these two fixed points have to move towards each other as β is increased. They have to vanish before $\beta = 1$, as g_1 has no fixed points, and the only possibility to do so is to collide at a unique bifurcation parameter β_c.

(b) If $\mathbb{T} = \mathbb{Z}$ (that is, in the discrete time case), the simplest way to obtain a reference family of this kind is to fix some strictly increasing map $g : \mathbb{R} \to \mathbb{R}$ such that g maps the points $\gamma^\pm$ below themselves, is strictly concave on $[\gamma^-, \gamma^+]$ and has two fixed points in $[\gamma^-, \gamma^+]$,

but $g-1$ does not have any fixed points in this interval. Then $g_\beta = g-\beta$ satisfies the above properties.

Our main result of this section now states that under some mild conditions, any random perturbation of such a reference family will undergo a non-smooth fold bifurcation.

Theorem 3.4. *Suppose that $(\Theta, \mathcal{B}, \nu, \omega)$ is an mpds and $(\Xi_\beta)_{\beta\in[0,1]}$ is a parameter family of ω-forced monotone flows that satisfies the assumptions of theorem 2.5 with constant curves $\gamma^\pm$. Further, assume that $(g_\beta)_{\beta\in[0,1]}$ is an autonomous reference family such that the following conditions hold for all $\beta\in[0,1]$.*

(a) For all $x\in X$, $t>0$ and ν-almost all $\theta\in\Theta$ we have $g^t_\beta(x)\leqslant\xi^t_\beta(\theta,x)$. (Lower bound)

(b) For all $\varepsilon, T>0$ there exists a set $A_{\varepsilon,T}\subseteq\Theta$ of positive measure $\nu(A_{\varepsilon,T})>0$ such that

$$|\xi^t_\beta(\theta,x)-g_\beta(x)| \leqslant \varepsilon \quad\text{and}\quad |\partial_x\xi^t_\beta(\theta,x)-\partial_x g^t_\beta(x)| \leqslant \varepsilon \tag{35}$$

for all $\theta\in A_{\varepsilon,T}$, $|t|\leqslant T$ and $x\in[\gamma^-,\gamma^+]$. (Shadowing)

(c) For ν-almost every $\theta\in\Theta$ there exists $t\in\mathbb{T}$ and $\delta>0$ such that $\xi^t_\beta(\omega^{-t}(\theta),x)\geqslant g^t_\beta(x)+\delta$ for all $x\in[\gamma^-,\gamma^+]$. (Separation)

Then $(\Xi_\beta)_{\beta\in[0,1]}$ undergoes a non-smooth fold bifurcation and the bifurcation parameter β_c is the same as in the reference family $(g_\beta)_{\beta\in[0,1]}$.

Remark 3.5. Note that by construction the forced Allee model (22) with random forcing term (4) satisfies the assumptions of theorem 3.4, with the unforced Allee model as a reference family. This then implies theorem 2.

In order to prove theorem 3.4, we first provide the following auxiliary statement about the equivalence of the existence of invariant graphs and the existence of orbits that remain in the region $\Gamma=\Theta\times[-\gamma,\gamma]$ at all times.

Lemma 3.6. *Suppose Ξ is a monotone skew product flow of the form (5) with an mpds $(\Theta,\mathcal{B},\nu,\omega)$ in the base. Further, assume that there exist measurable curves $\gamma^-\leqslant\gamma^+:\Theta\to X$ that satisfy*

$$\xi^t(\theta,\gamma^\pm(\theta)) \leqslant \gamma^\pm(\omega(\theta)) \tag{36}$$

for ν-almost every $\theta\in\Theta$ and all $t\geqslant 0$. Let

$$\Gamma=\{(\theta,x)|\theta\in\Theta,\ \gamma^-(\theta)\leqslant x\leqslant\gamma^+(\theta)\}. \tag{37}$$

Then there exists a (Ξ,ν)-invariant graph φ in Γ if and only if

$$\xi^t(\theta,\gamma^+(\theta)) \geqslant \gamma^-(\omega^t(\theta)) \tag{38}$$

holds for all $t\geqslant 0$ and ν-almost every $\theta\in\Theta$.

Proof An important ingredient for the proof are the *graph transforms* $\Xi^t_*\gamma$ of a measurable function $\gamma:\Theta\to X$. For $t\in\mathbb{T}$, these are defined by

$$\Xi^t_*\gamma(\theta)=\xi^t(\omega^{-t}(\theta),\gamma(\omega^{-t}(\theta))). \tag{39}$$

If $t \geqslant 0$, we speak of a *forwards transform* and if $t \leqslant 0$, of a *backwards transform*. We define

$$\gamma_t^+ = \Xi_*^t \gamma^+ \quad \text{and} \quad \gamma_t^- = \Xi_*^{-t} \gamma^-. \tag{40}$$

Then (36) together with the monotonicity of the fibre maps implies that the family of functions γ_t^+ is decreasing in t. Similarly, the family γ_t^- is increasing (note here that $\xi^t(\theta, \gamma^-(\theta)) \leqslant \gamma^-(\theta)$ for $t > 0$ implies $\xi^t(\theta, \gamma^-(\theta)) \geqslant \gamma^-(\theta)$ for $t < 0$).

Suppose now that (38) holds for all $t > 0$ and ν-almost every $\theta \in \Theta$. Then γ_t^+ is bounded below by γ^- for all $t > 0$ and thus converges ν-almost everywhere to a function

$$\varphi^+(\theta) = \lim_{t\to\infty} \gamma_t^+(\theta). \tag{41}$$

Due to the continuity of the fibre maps, we have that

$$\begin{aligned} \xi^s(\theta, \varphi^+(\theta)) &= \xi^s\left(\theta, \lim_{t\to\infty} \gamma_t^+(\theta)\right) = \lim_{t\to\infty} \xi^s(\theta, \gamma_t^+(\theta)) \\ &= \lim_{t\to\infty} \gamma_{t+s}^+(\omega^s(\theta)) = \varphi^+(\omega^s(\theta)) \end{aligned} \tag{42}$$

ν-almost everywhere. Hence, φ^+ is the desired invariant graph.

Conversely, assume that there exists an invariant graph φ in Γ. Then the monotonicity of the fibre maps gives

$$\xi^t(\theta, \gamma^+(\theta)) \geqslant \xi^t(\theta, \varphi(\theta)) = \varphi(\omega^t(\theta)) \ \geqslant \ \gamma^-(\omega^t(\theta)) \tag{43}$$

for ν-almost every $\theta \in \Theta$. □

Remark 3.7. As we have seen in the above proof, if Ξ satisfies the assumptions of lemma 3.6 and has at least one invariant graph, then the formula

$$\varphi^+(\theta) = \lim_{t\to\infty} \gamma_t^+(\theta) = \lim_{t\to\infty} \xi^t(\omega^{-t}(\theta), \gamma^+(\omega^{-t}(\theta))) \tag{44}$$

yields one such graph. This way of defining an invariant graph is called *pullback construction* and generally works if the graph is an attractor. In a similar fashion, it is possible to show that the *pushforward construction*

$$\varphi^-(\theta) = \lim_{t\to-\infty} \gamma_t^-(\theta) = \lim_{t\to\infty} \xi^{-t}(\omega^t(\theta), \gamma^-(\omega^t(\theta))) \tag{45}$$

also defines an invariant graph, which usually is a repeller. However, the graphs φ^- and φ^+ may coincide, as in the case of a smooth fold bifurcation (see theorem 2.5).

We can now turn to the

Proof of Theorem 3.4. Let β_c be the bifurcation parameter for the family $(\Xi_\beta)_{\beta\in[0,1]}$ and $\tilde{\beta}_c$ the one for the reference family $(g_\beta)_{\beta\in[0,1]}$. We first show that $\beta_c = \tilde{\beta}_c$. Denote the unique fixed point of $g_{\tilde{\beta}_c}$ in $[\gamma^-, \gamma^+]$ by x_0. Then, for ν-almost all $\theta \in \Theta$ and all $\beta < \tilde{\beta}_c$ and $t \geqslant 0$, we obtain

$$\xi_\beta^t(\theta, \gamma^+) \ \geqslant \ \xi_{\tilde{\beta}_c}^t(\theta, \gamma^+) \ \geqslant \ g_{\tilde{\beta}_c}^t(\gamma^+) \ \geqslant \ g_{\tilde{\beta}_c}^t(x_0) = x_0 \ \geqslant \ \gamma^-.$$

Hence, lemma 3.6 implies that Ξ_β has at least one invariant graph in Γ for all $\beta \leqslant \tilde{\beta}_c$, and thus $\beta_c \geqslant \tilde{\beta}_c$.

Conversely, suppose that $\beta > \tilde{\beta}_c$. As g_β has no fixed points in $[\gamma^-, \gamma^+]$ and $g^t_\beta(\gamma^+) < \gamma^+$ for all $t \geqslant 0$, we obtain that $g^T_\beta(\gamma^+) < \gamma^-$ for some $T > 0$. Let $\varepsilon > 0$ be such that $g^T_\beta(\gamma^+) < \gamma^- - \varepsilon$. By assumption, the set $A_{\varepsilon,T}$ in the statement of the theorem has positive measure. For any $\theta \in A_{\varepsilon,T}$, we obtain

$$\xi^T_\beta(\theta, \gamma^+) \;\leqslant\; g^T_\beta(\gamma^+) + \varepsilon \;<\; \gamma^-.$$

Due to lemma 3.6, this excludes the existence of an invariant graph in Γ for $\beta > \beta_c$. We therefore obtain $\beta_c \leqslant \tilde{\beta}_c$. Together with the above, this yields $\beta_c = \tilde{\beta}_c$.

It remains to show the non-smoothness of the bifurcation. To that end, we set

$$\varphi^+(\theta) = \lim_{t\to\infty} \xi^t_{\beta_c}(\omega^{-t}(\theta), \gamma^+) \quad \text{and} \quad \varphi^-(\theta) = \lim_{t\to\infty} \xi^{-t}_{\beta_c}(\omega^t(\theta), \gamma^-).$$

As discussed in remark 3.7, φ^+ and φ^- are well-defined invariant graphs. To finish the proof, we have to show that $\varphi^-(\theta) < \varphi^+(\theta)\nu$-almost surely.

To that end, observe that condition (a) in theorem 3.4 together with the monotonicity of the fibre maps implies $\xi^t_{\beta_c}(\theta, x) \leqslant g^t_{\beta_c}(x)$ for all $x \in [\gamma^-, \gamma^+]$, all $t < 0$ and ν-almost all $\theta \in \Theta$. As a consequence, we have $\varphi^-(\theta) \leqslant x_0$ almost surely. Now, by assumption (c) we have that for ν-almost every $\theta \in \Theta$ there exists $\delta > 0$ and $s \in \mathbb{T}$ such that $\xi^s_{\beta_c}(\omega^{-s}(\theta), x_0) > g^s_{\beta_c}(x_0) + \delta = x_0 + \delta$. Thus, we obtain

$$\begin{aligned}\varphi^+(\theta) &= \lim_{t\to\infty} \xi^t_{\beta_c}(\omega^{-t}(\theta), \gamma^+) \\ &= \lim_{t\to\infty} \xi^s_{\beta_c}(\omega^{-s}(\theta), \xi^{t-s}_{\beta_c}(\omega^{-t}(\theta), \gamma^+)) \geqslant \lim_{t\to\infty} \xi^s_{\beta_c}(\omega^{-s}(\theta), g^{t-s}_{\beta_c}(\gamma^+)) \\ &\geqslant \xi^s_{\beta_c}(\omega^{-s}(\theta), x_0) \;\geqslant\; x_0 + \delta\end{aligned}$$

and hence, in particular, $\varphi^+(\theta) > x_0 \geqslant \varphi^-(\theta)$. This finishes the proof. □

4. Lyapunov exponents in nonsmooth fold bifurcations

4.1. Lyapunov gap in nonsmooth fold bifurcations

The aim of this section is to provide a proof of theorem 1, which we restate here in a more general form.

Theorem 4.1. *Suppose that $(\Xi_\beta)_{\beta\in[0,1]}$ is a parameter family of forced monotone $\mathcal{C}^2$-flows that satisfies the assumptions of theorem 2.2 (for deterministic forcing) or theorem 2.5 (for random forcing). Further, assume that the fold bifurcation that occurs in this family at the critical parameter β_c is non-smooth. Then*

$$\lim_{\beta\nearrow\beta_c} \lambda(\varphi^+_\beta) = \lambda(\varphi^+_{\beta_c}) \;<\; 0. \tag{46}$$

If the fold bifurcation is smooth, then $\lim_{\beta\nearrow\beta_c} \lambda(\varphi^+_\beta) = 0$. The analogous results hold for the unstable equilibrium φ^-_β.

Proof. Let us first consider the deterministic case, that is, assume $(\Xi_\beta)_{\beta\in[0,1]}$ satisfies the assumptions of theorem 2.2. We claim that for each $\theta \in \Theta$ we have that $\varphi^+_{\beta_c}(\theta)$ coincides with

$$\varphi(\theta) = \lim_{\beta\nearrow\beta_c} \varphi^+_\beta(\theta).$$

Note that φ is well-defined due to the monotone dependence of ξ^t_β on β (see assumption (e) in theorem 2.2) which results in $\varphi_\beta \geqslant \varphi_{\beta'}$ whenever $\beta < \beta' \leqslant \beta_c$.

In order to see that φ is an invariant graph, fix $\theta \in \Theta$, $t > 0$ and $\varepsilon > 0$. Choose $\delta > 0$ such that $|\xi^t_{\beta_c}(\theta, \varphi(\theta)) - \xi^t_{\beta_c}(\theta, x)| < \varepsilon$ for all $x \in B_\delta(\varphi(\theta))$ and at the same time $|\xi^t_\beta(\theta, x) - \xi^t_{\beta'}(\theta, x)| < \varepsilon$ whenever $|\beta - \beta'| < \delta$. Note that such δ exists due to the uniform continuity of $(\beta, x) \mapsto \xi^t_\beta(\theta, x)$. Let $\beta < \beta_c$ be such that $\beta_c - \beta < \delta$, $\varphi^+_\beta(\theta) - \varphi(\theta) < \delta$ and $\varphi^+_\beta(\omega^t(\theta)) - \varphi(\omega^t(\theta)) < \varepsilon$. We obtain

$$\begin{aligned} |\xi^t_{\beta_c}(\theta, \varphi(\theta)) - \varphi(\omega^t(\theta))| &\leqslant |\xi^t_\beta(\theta, \varphi(\theta)) - \varphi^+_\beta(\omega^t(\theta))| + 2\varepsilon \\ &= |\xi^t_\beta(\theta, \varphi(\theta)) - \xi^t_\beta(\theta, \varphi^+_\beta(\theta))| + 2\varepsilon \leqslant 3\varepsilon. \end{aligned}$$

As $\varepsilon > 0$ was arbitrary, this proves $\xi^t_{\beta_c}(\theta, \varphi(\theta)) = \varphi(\omega^t(\theta))$ and hence the invariance of φ under Ξ_{β_c}. Now, since the graphs $\varphi^+_{\beta_c}$ are monotonically decreasing in β, we have $\varphi \geqslant \varphi^+_{\beta_c}$. As there is no Ξ_{β_c}-invariant graph above $\varphi^+_{\beta_c}$ in the considered region Γ, we obtain $\varphi^+_{\beta_c} = \varphi$. Using dominated convergence, this proves the statement about the Lyapunov exponents in the deterministic case.

In the random case, the above arguments (applied to almost every θ instead of every θ) work similarly (when using theorem 2.5 instead of theorem 2.2). □

4.2. Slope at the bifurcation point

Although this is not in our main focus, we want to comment in this section on a particular qualitative difference between non-smooth fold bifurcations in the qpf and the rdf case. As it can be seen from figures 2(b)–(d), the slope of the Lyapunov exponent of the attractor increases strongly towards the bifurcation in the qpf case, whereas it only increases slightly or even remains constant in the random case.

In fact, the heuristic description of non-smooth fold bifurcations in qpf systems given in section 2.5 suggests that $\partial_\beta \lambda(\varphi^+_\beta)$ should actually increase to infinity as $\beta \nearrow \beta_c^+$. The reason is that due to the concavity of the right side of the vector field, the Lyapunov exponent increases whenever the graph decreases. Thereby, the quantitative contribution of each peak that develops should be the product between its width and its speed, which is more or less constant since both decrease, respectively increase, with the same exponential rate. Hence, every peak contributes a similar amount to the slope of the Lyapunov exponent, and as there are infinitely many peaks, this slope grows to infinity as the bifurcation is approached. In principle, we believe that this heuristic explanation could be made precise by using the machinery for the proof of non-smooth fold bifurcations in [Fuh16a, Fuh16b] which, however, goes beyond our current scope.

For the case of random forcing, we provide a proof for the boundedness of the slope of the Lyapunov exponent of φ^+_β as $\beta \nearrow \beta_c$. In order to avoid too many technicalities and to not obstruct the view on the underlying mechanism, we restrict to the case of the discrete-time example (26). We note, however, that the proof can be generalised to broader classes of monotone skew product maps and, with some more work required, to continuous-time systems.

Theorem 4.2. *Suppose $(f_\beta)_{\beta\in[0,1]}$ is the family of skew product maps given by (26) with $\Theta = \{0, 1\}^{\mathbb{Z}}$ the Bernoulli space equipped with the shift map σ and the Bernoulli measure μ. Let $\beta_c = \arctan(\sqrt{\alpha - 1}) - \sqrt{\alpha - 1}/\alpha - \kappa$. Then $(f_\beta)_{\beta\in[0,1]}$ satisfies the hypothesis of theorem 2.5 (with $\gamma^- = 0$ and $\gamma^+ = \pi/2$) and undergoes a non-smooth saddle-node bifurcation with*

critical parameter β_c. *Moreover, there exists a constant* $C > 0$ *such that*

$$|\partial_\beta \lambda_\mu(\varphi^\pm_\beta)| \leqslant C$$

for all $\beta \in [0, \beta_c]$.

Before we turn to the proof of the theorem 4.2, we first need the following preliminary result.

Lemma 4.3. *In the situation of theorem 4.2 we let* $\gamma^\pm_{n,\beta} = f^{\pm n}_{\beta *}\gamma^\pm$, *where the graph transform* $f^n_{\beta *}$ *is defined as in the proof of theorem 3.6. Then* $\gamma^\pm_{n,\beta}(\theta)$ *converges to* $\varphi^\pm_\beta(\theta)$ *uniformly in* β *and* θ (*with* $\beta \in [0, \beta_c]$ *and* $\theta \in \Sigma$) *as* $n \to \infty$.

Moreover, for all $\theta \in \Sigma$, *the map* $[0, \beta_c) \ni \beta \mapsto \varphi^\pm_\beta(\theta)$ *is differentiable and for every* $\beta' \in [0, \beta_c)$, *we have that*

$$\partial_\beta \gamma^\pm_{n,\beta}(\theta) = -\sum_{i=1}^{n} \prod_{\ell=1}^{i-1} \partial_x f^{\pm 1}{}_{\beta,\sigma^{-\ell}\theta}(f^{\pm(n-\ell)}_{\beta,\sigma^{-n}\theta}(\gamma^+)) \xrightarrow{n\to\infty} \partial_\beta \varphi^\pm_\beta(\theta) \tag{47}$$

uniformly in β *and* θ *for all* $\beta \in [0, \beta']$ *and all* $\theta \in \Sigma$.

Proof. We only consider $\gamma^+_{n,\beta}$ and φ^+_β, the statements for $\gamma^-_{n,\beta}$ and φ^-_β follow analogously. Recall that

$$f_\beta : \Sigma \times \mathbb{R} \to \Sigma \times \mathbb{R}, \quad (\theta, x) \mapsto (\omega(\theta), g(x) - \kappa \cdot \theta_0 - \beta),$$

with $g(x) = \arctan(\alpha x)$.

First, observe that $\partial_x^2 f^n_{\beta,\theta}(x) < 0$ for all $n \in \mathbb{N}$ as long as $x, f_{\beta,\theta}(x), \ldots, f_{\beta,\omega^{n-1}(\theta)}(x) > 0$ since the composition of concave increasing functions is again concave. Second, note that with $\theta^* = \ldots\ 1, 1, 1 \ldots \in \Sigma$, we have

$$f_{\beta_c,\theta^*}(x) = f_{\beta,\theta}(x) - (\beta_c - \beta) - \kappa(1 - \theta_0) \tag{48}$$

for all $\beta \in [0, \beta_c]$ and all $\theta \in \Sigma, x \in X$.

Hence, we obtain that for all $\beta \in [0, \beta_c], \theta \in \Sigma$ and all $n, n' \in \mathbb{N}$ with $n \geqslant n'$ we have

$$\begin{aligned}
|\gamma^+_{n',\beta}(\theta) - \gamma^+_{n,\beta}(\theta)| &= f^{n'}_{\beta,\sigma^{-n'}\theta}(\gamma^+) - f^{n'}_{\beta,\sigma^{-n'}\theta}(f^{n-n'}_{\beta,\sigma^{-n}\theta}(\gamma^+)) \\
&\leqslant f^{n'}_{\beta,\sigma^{-n'}\theta}(\gamma^+) - f^{n'}_{\beta,\sigma^{-n'}\theta}(f^{n-n'}_{\beta_c,\theta^*}(\gamma^+)) \\
&= f^{n'-1}_{\beta,\sigma^{1-n'}\theta}(f_{\beta,\sigma^{-n'}\theta}(\gamma^+)) - f^{n'-1}_{\beta,\sigma^{1-n'}\theta}(f_{\beta,\sigma^{-n'}\theta}(f^{n-n'}_{\beta_c,\theta^*}(\gamma^+))) \\
&\leqslant f^{n'-1}_{\beta,\sigma^{1-n'}\theta}(f_{\beta_c,\theta^*}(\gamma^+)) - f^{n'-1}_{\beta,\sigma^{1-n'}\theta}(f_{\beta_c,\theta^*}(f^{n-n'}_{\beta_c,\theta^*}(\gamma^+))) \\
&\leqslant f^{n'-2}_{\beta,\sigma^{2-n'}\theta}(f^2_{\beta_c,\theta^*}(\gamma^+)) - f^{n'-2}_{\beta,\sigma^{2-n'}\theta}(f^2_{\beta_c,\theta^*}(f^{n-n'}_{\beta_c,\theta^*}(\gamma^+))) \\
&\leqslant \ldots \leqslant f^{n'}_{\beta_c,\theta^*}(\gamma^+) - f^{n'}_{\beta_c,\theta^*}(f^{n-n'}_{\beta_c,\theta^*}(\gamma^+)) \\
&= |\gamma^+_{n',\beta_c}(\theta^*) - \gamma^+_{n,\beta_c}(\theta^*)|,
\end{aligned}$$

where we used the monotonicity of the fibre maps in the first inequality and the above mentioned concavity together with (48) in the steps to the fourth, fifth and sixth line. This proves the first part.

Next, we show that $\partial_\beta \gamma^+_{n,\beta}(\theta)$ converges uniformly in θ and β which immediately implies the second part. To that end, we first provide a uniform upper bound on

$$\sup_{\theta\in\Sigma,\beta\in[0,\beta']} \partial_x f_{\beta,\theta}(\gamma^+_{n,\beta}(\theta))$$

for all $n \in \mathbb{N}$. Similarly as in the proof of theorem 3.4, we see that

$$x_{\min}(\beta) \;:=\; \min_{\theta\in\Sigma} \varphi^+_\beta(\theta) \geqslant x_0(\beta')$$

for all $\beta \in [0, \beta']$, where $x_0(\beta')$ is the upper fixed point of the map $g - \kappa - \beta'$. Hence, we have

$$\begin{aligned} 0 \leqslant \sup_{\theta\in\Sigma,\beta\in[0,\beta']} \partial_x f_{\beta,\theta}(\gamma^+_{n,\beta}(\theta)) &= \sup_{\theta\in\Sigma,\beta\in[0,\beta']} g'(\gamma^+_{n,\beta}(\theta)) \;\leqslant\; g'(\varphi^+_\beta(\theta)) \\ &\leqslant\; g'(x_0(\beta')) \;=:\; c \;<\; 1, \end{aligned} \tag{49}$$

where we used the concavity of g and the monotone dependence of $\varphi^+_\beta(\theta)$ on β.

Now, observe that

$$\begin{aligned} \partial_\beta \gamma^+_{n,\beta}(\theta) =\; & \partial_\beta f^n_{\beta,\sigma^{-n}\theta}(\gamma^+) \\ &= \partial_\beta f_{\beta,\sigma^{-1}\theta}(f^{n-1}_{\beta,\sigma^{-n}\theta}(\gamma^+)) \\ &\quad + \partial_x f_{\beta,\sigma^{-1}\theta}(f^{n-1}_{\beta,\sigma^{-n}\theta}(\gamma^+)) \cdot \partial_\beta f^{n-1}_{\beta,\sigma^{-n}\theta}(\gamma^+) \\ &= \ldots = \sum_{i=1}^{n} \partial_\beta f_{\beta,\sigma^{-i}\theta}(f^{n-i}_{\beta,\sigma^{-n}\theta}(\gamma^+)) \prod_{\ell=1}^{i-1} \partial_x f_{\beta,\sigma^{-\ell}\theta}(f^{n-\ell}_{\beta,\sigma^{-n}\theta}(\gamma^+)) \\ &= -\sum_{i=1}^{n} \prod_{\ell=1}^{i-1} \partial_x f_{\beta,\sigma^{-\ell}\theta}(f^{n-\ell}_{\beta,\sigma^{-n}\theta}(\gamma^+)). \end{aligned}$$

Together with (49), we hence obtain for $n \geqslant n'$

$$\begin{aligned} |\partial_\beta \gamma^+_{n',\beta}(\theta) - \partial_\beta \gamma^+_{n,\beta}(\theta)| &= \sum_{i=n'+1}^{n} \prod_{\ell=1}^{i-1} \partial_x f_{\beta,\sigma^{-\ell}\theta}(f^{n-\ell}_{\beta,\sigma^{-n}\theta}(\gamma^+)) \\ &\leqslant \sum_{i=n'+1}^{n} c^{i-1}, \end{aligned}$$

which proves the statement. □

We can now turn to the

Proof of Theorem 4.2. We keep the notation as in the previous proof. Observe that $(g - \kappa - \beta)_{\beta\in[0,1]}$ is an autonomous reference family for $(f_\beta)_{\beta\in[0,1]}$. Therefore, the fact that

$(f_\beta)_{\beta\in[0,1]}$ undergoes a non-smooth saddle-node bifurcation with critical parameter β_c (given by the bifurcation parameter of the family $(g-\kappa-\beta)_\beta$) is a direct consequence of theorem 3.4. Hence, it remains to prove the existence of a uniform bound on the slope of the Lyapunov exponent. As before, we only consider φ_β^+. Further, we show the statement for $\beta\in[0,\beta_c)$ which immediately yields the full statement by means of the mean value theorem.

Given $\beta\in[0,\beta_c)$, observe that

$$\begin{aligned}\partial_\beta\lambda_\mu(\varphi_\beta^+) &= \partial_\beta\int_\Sigma \log\partial_x f_{\beta,\theta}(\varphi_\beta^+(\theta))\,d\theta\\ &= \partial_\beta\int_\Sigma \log g'(\varphi_\beta^+(\theta))\,d\theta = \int_\Sigma \frac{g''(\varphi_\beta^+(\theta))}{g'(\varphi_\beta^+(\theta))}\cdot\partial_\beta\varphi_\beta^+(\theta)\,d\theta.\end{aligned}$$

With $c\geqslant\sup_{x\in[0,\pi/2]}|g''(x)/g'(x)|$, we hence obtain

$$|\partial_\beta\lambda_\mu(\varphi_\beta^+)|\leqslant c\int_\Sigma|\partial_\beta\varphi_\beta^+(\theta)|\,d\theta.$$

Now, let

$$\alpha=\sup_{\theta\in\Sigma,\,\theta_0=0} f'_{\beta_c,\sigma\theta}(f_{\beta_c,\theta}(x_c))$$

and note that

$$\alpha=g'(g(x_c)-\beta_c)=g'(g(x_c)-\kappa-\beta_c+\kappa)=g'(x_c+\kappa)\;<\;g'(x_c)=1,$$

where x_c is the neutral fixed point of the map $g-\kappa-\beta_c$. Then

$$\begin{aligned}\int_\Sigma|\partial_\beta\varphi_\beta^+(\theta)|\,d\theta &= \int_\Sigma|\partial_\beta\lim_{n\to\infty}\gamma_{n,\beta}^+(\theta)|\,d\theta = \lim_{n\to\infty}\int_\Sigma|\partial_\beta\gamma_{n,\beta}^+(\theta)|\,d\theta\\ &\overset{(47)}{=}\lim_{n\to\infty}\int_\Sigma\sum_{i=1}^n\prod_{\ell=1}^{i-1}\partial_x f_{\beta,\sigma^{-\ell}\theta}(f_{\beta,\sigma^{-n}\theta}^{n-\ell}(\gamma^+))\,d\theta\\ &=\lim_{n\to\infty}\sum_{i=1}^n\int_\Sigma\prod_{\ell=1}^{i-1}\partial_x f_{\beta,\sigma^{-\ell}\theta}(f_{\beta,\sigma^{-n}\theta}^{n-\ell}(\gamma^+))\,d\theta\\ &\leqslant\lim_{n\to\infty}\sum_{i=1}^n\int_\Sigma\prod_{\ell=1}^{i-1}\partial_x f_{\beta,\sigma^{-\ell}\theta}(f_{\beta,\sigma^{-\ell-1}\theta}(x_c))\,d\theta\\ &\leqslant\lim_{n\to\infty}\sum_{i=1}^n\sum_{k=0}^{i-1}\alpha^k\cdot\mu\big(\{\theta\in\Sigma:k=\#\{1<\ell\leqslant i:\theta_{-\ell}=0\}\}\big)\\ &=\lim_{n\to\infty}\sum_{i=1}^n\sum_{k=0}^{i-1}\alpha^k\cdot\binom{i-1}{k}(1/2)^{i-1}\\ &=\lim_{n\to\infty}\sum_{i=1}^n\sum_{k=0}^{i-1}\binom{i-1}{k}(\alpha/2)^k(1/2)^{i-1-k}\\ &=\lim_{n\to\infty}\sum_{i=1}^n(\alpha/2+1/2)^{i-1}<\infty.\end{aligned}$$

Since α is independent of β, the statement follows. □

5. Range of finite-time Lyapunov exponents

In this section, we provide a proof of theorem 3, which we restate below in a more general form. To that end, let us introduce the maximal finite-time Lyapunov exponents on the attractor. As invariant graphs only need to be defined almost surely, we just take into account exponents that can be 'seen' on a set of positive measure by setting

$$\lambda_k^{\max}(\varphi_\beta^+) = \sup\left\{\lambda \in \mathbb{R}\middle|\mu_{\varphi_\beta^+}(\{(\theta,x)|\lambda_k(f_\beta,\theta,x) \geqslant \lambda\}) > 0\right\}.$$

Here, the graph measure $\mu_{\varphi_\beta^+}$ is as discussed in section 2.1. Note that if the forcing is quasiperiodic, then the attractors prior to the bifurcation are all continuous so that we actually have $\lambda_k^{\max}(\varphi_\beta^+) = \max\left\{\lambda_k(\theta,\varphi_\beta^+(\theta))\middle|\theta \in \mathbb{T}^1\right\}$ whenever $\beta < \beta_c$.

We first consider the case of quasiperiodic forcing, where the general statement we aim at reads as follows.

Theorem 5.1. *Suppose $(\Xi_\beta)_{\beta\in[0,1]}$ is a parameter family of qpf monotone flows that satisfies the hypotheses of theorem 2.2. Then for all $k \in \mathbb{N}$ we have*

$$\varliminf_{\beta\nearrow\beta_c} \lambda_k^{\max}(\varphi_\beta^+) \;\geqslant\; \lambda(\varphi_{\beta_c}^-). \tag{50}$$

Before we turn to the proof, however, we have to address some subtleties concerning the topology of pinched invariant graphs in this setting. Suppose we observe a non-smooth bifurcation as characterised in theorem 2.2, so that there exist exactly two graphs $\varphi_{\beta_c}^- < \varphi_{\beta_c}^+$ (up to modifications on sets of measure zero), where $\varphi_{\beta_c}^-$ is lower and $\varphi_{\beta_c}^+$ is upper semicontinuous. Let $A^+ = \operatorname{supp}(\mu_{\varphi_{\beta_c}^+})$ and $A^- = \operatorname{supp}(\mu_{\varphi_{\beta+}^-})$, where $\operatorname{supp}(\nu)$ denotes the topological support of a measure ν.[12] Then A^+ is Ξ_{β_c}-invariant, and consequently the upper and lower bounding graphs $\varphi_{A^+}^{\mathrm{u}}$ and $\varphi_{A^+}^{\mathrm{l}}$ given by

$$\varphi_{A^+}^{\mathrm{u}}(\theta) = \sup A_\theta^+ \quad \text{and} \quad \varphi_{A^+}^{\mathrm{l}}(\theta) = \inf A_\theta^+$$

are Ξ_β-invariant graphs, with $\varphi_{A^+}^{\mathrm{u}}$ upper and $\varphi_{A^+}^{\mathrm{l}}(\theta)$ lower semicontinuous (see [Sta03]). As $\varphi_{\beta_c}^\pm$ are the only Ξ_β-invariant graphs in the considered region Γ, we must have $\varphi_{A^+}^{\mathrm{l}}(\theta) = \varphi_{\beta_c}^-$ and $\varphi_{A^+}^{\mathrm{u}} = \varphi_{\beta_c}^+$ almost surely (see [Sta03] for more details), but the graphs may differ on a set of measure zero (which is the subtle complication that requires particular care in the proof of theorem 5.1 below). Nevertheless, this implies in particular that $(\theta,\varphi_{\beta_c}^-(\theta)) \in A^+$ almost surely, so that $\mu_{\varphi_{\beta_c}^-}(A^+) = 1$ and hence $A^- \subseteq A^+$. As the converse inclusion follows in the same way, we have $A^- = A^+$. One particular consequence of this discussion is the following

[12] Given a Borel measure ν on some second countable metric space X, the support of ν is defined as $\operatorname{supp}(\nu) = \{x \in X|\nu(B_\delta(x)) > 0 \forall\, \delta > 0\} = X\backslash\bigcup_{U \text{ open},\, \nu(U)=0} U$. It is easy to see that $\operatorname{supp}(\nu)$ is always closed and can be characterised as the smallest closed set $A \subseteq X$ with $\nu(X\backslash A) = 0$. Moreover, if ν is invariant under some continuous transformation f, then so is $\operatorname{supp}(\nu)$.

Lemma 5.2. *For μ-almost every $\theta_0 \in \Theta$ and every $\delta > 0$ there exists a set $B \subseteq \Theta$ of positive measure such that*

$$\{(\theta, \varphi^+_{\beta_c}(\theta)) | \theta \in B\} \subseteq B_\delta((\theta_0, \varphi^-_{\beta_c}(\theta_0))).$$

We can now turn to the

Proof of Theorem 5.1. Fix $k \in \mathbb{N}$. First, we claim that there exists a set of positive measure of $\theta \in \Theta$ such that

$$\lambda_k(\theta, \varphi^-_{\beta_c}(\theta)) \geqslant \lambda(\varphi^-_{\beta_c}). \tag{51}$$

In order to see this, assume for a contradiction that $\lambda_k(\theta, \varphi^-_{\beta_c}(\theta)) < \lambda(\varphi^-_{\beta_c})$ for almost all θ. Clearly, this implies the existence of $\delta > 0$ and of a set $\Theta_\delta \subseteq \Theta$ of positive measure such that

$$\lambda_k(\theta, \varphi^-_{\beta_c}(\theta)) \leqslant \lambda(\varphi^-_{\beta_c}) - \delta$$

for all $\theta \in \Theta_\delta$. Due to Birkhoff's ergodic theorem (and the ergodicity of the flow ω on Θ), the orbit of almost every $\theta \in \Theta$ visits the set Θ_δ with positive frequency. This implies that the pointwise Lyapunov exponent of almost every θ satisfies

$$\lambda(\theta, \varphi^-_{\beta_c}(\theta)) < \lambda(\varphi^-_{\beta_c}).$$

This, however, contradicts Birkhoff's ergodic theorem according to which we have

$$\lambda(\theta, \varphi^-_{\beta_c}(\theta)) = \lambda(\varphi^-_{\beta_c})$$

almost surely. Hence, there exists a positive measure set of θ which satisfies (51).

Now, let $\varepsilon > 0$ be given. Due to lemma 5.2, there is $\delta > 0$ and $\theta_0 \in \Theta$ which satisfies (51) and a set $B \subseteq \Theta$ of positive measure such that $(\theta, \varphi^+_{\beta_c}(\theta)) \in B_\delta(\theta_0, \varphi^-_{\beta_c}(\theta_0))$ for all $\theta \in B$. If δ is chosen small enough, then it follows by continuity that

$$\lambda_k(\theta, \varphi^+_{\beta_c}(\theta)) \geqslant \lambda(\varphi^-_{\beta_c}) - \varepsilon$$

for all $\theta \in B$. As $\varepsilon > 0$ was arbitrary, we obtain that $\lambda^{\max}_k(\varphi^+_{\beta_c}) \geqslant \lambda(\varphi^-_{\beta_c})$. Finally, as $\lim_{\beta \nearrow \beta_c} \varphi^+_\beta(\theta) = \varphi^+_{\beta_c}(\theta)$ almost surely (see the proof of theorem 4.1), we obtain (50) again by continuity. □

We now turn to the random case. In this case, we have to restrict to the setting of theorem 3.4 (instead of the more general situation of theorem 2.5).

Theorem 5.3. *Suppose that $(\Xi_\beta)_{\beta \in [0,1]}$ is a parameter family of randomly forced monotone flows that satisfies the assumptions of theorem 3.4. Then for all $k \in \mathbb{R}$*

$$\lim_{\beta \nearrow \beta_c} \lambda^{\max}_k(\varphi^+_\beta(\theta)) = 0.$$

Proof. Let $(g_\beta)_{\beta \in [0,1]}$ be the autonomous reference family from theorem 3.4. Then we have that g_{β_c} has a unique fixed point $x_0 \in [\gamma^-, \gamma^+]$ whose Lyapunov exponent vanishes, that is, $\log \partial_t g^t_{\beta_c}(x_0) = 0$ for all $t > 0$. By continuity, this means that given $t \in \mathbb{R}$ and $\varepsilon > 0$ there exists $\delta > 0$ such that $|x - x_0| < \delta$ and $|\beta - \beta_c| < \delta$ implies $|\log(g^t_\beta(x))|/t < \varepsilon$. Moreover, as

$\lim_{t\to\infty} g^t_{\beta_c}(\gamma^+) = x_0$, we can further require that $g^t_\beta(\gamma^+) < x_0 + \delta/2$ for all $\beta \in [\beta_c - \delta', \beta_c]$ and some $t, \delta' > 0$.

Now, by assumption (b) of theorem 3.4 there exists a set $A_{\delta/2,t} \subseteq \Theta$ of positive measure such that for all $\theta \in \omega^t(A_{\delta/2,t})$ we have

$$\xi^t_\beta(\omega^{-t}(\theta), \gamma^+) \leqslant x_0 + \delta.$$

As $\varphi^+_\beta(\theta)$ is the monotone limit of the sequence $\xi^t_\beta(\omega^{-t}(\theta), \gamma^+)$ (see the proof of theorem 3.4) and is bounded below by x_0, this implies that $x_0 \leqslant \varphi^+_\beta(\theta) \leqslant x_0 + \delta$ and therefore, using condition (b) again, $|\lambda_t(\theta, \varphi^+_\beta(\theta))| < \varepsilon$ for all $\theta \in A_{\delta/2,k}$ and $\beta \in [\beta_c - \delta', \beta_c]$. As $\varepsilon > 0$ was arbitrary, this completes the proof. □

Acknowledgments

This project has received funding from the European Union's Horizon 2020 research and innovation program under the Marie Skłodowska-Curie Grant Agreements No. 643073 and No. 750865. TJ acknowledges support by a Heisenberg grant of the German Research Council (DFG Grant OE 538/6-1).

ORCID iDs

G Fuhrmann https://orcid.org/0000-0002-0634-0802
T Jäger https://orcid.org/0000-0001-8457-8392

References

[AJ02] Anagnostopoulou V and Jäger T 2012 Nonautonomous saddle-node bifurcations: random and deterministic forcing *J. Differ. Equ.* **253** 379–99
[Arn98] Arnold L 1998 *Random Dynamical Systems* (Berlin: Springer)
[Bje05] Bjerklöv K 2005 Dynamics of the quasiperiodic Schrödinger cocycle at the lowest energy in the spectrum *Commun. Math. Phys.* **272** 397–442
[Bje05b] Bjerklöv K 2005 Positive Lyapunov exponent and minimality for a class of one-dimensional quasi-periodic Schrödinger equations *Ergod. Theor. Dynam. Syst.* **25** 1015–45
[Bje07] Bjerklöv K 2007 Positive Lyapunov exponent and minimality for the continuous 1D quasi-periodic Schrödinger equation with two basic frequencies *Ann. Henri Poincare* **8** 687–730
[CCP+11] Carpenter S R *et al* 2011 Early warnings of regime shifts: a whole-ecosystem experiment *Science* **332** 1079–82
[DRC+89] Ditto W L *et al* 1989 Experimental observation of crisis-induced intermittency and its critical exponent *Phys. Rev. Lett.* **63** 923–6
[DSvN+08] Dakos V, Scheffer M, van Nes E H, Brovkin V V and Petoukhov H 2008 Slowing down as an early warning signal for abrupt climate change *Proc. Natl Acad. Sci. USA* **105** 14308–12
[FGJ18] Fuhrmann G, Gröger M and Jäger T 2018 Non-smooth saddle-node bifurcations II: dimensions of strange attractors *Ergod. Theor. Dynam. Syst.* **38** 2989–3011
[FJJK05] Fabbri R, Jäger T, Johnson R and Keller G 2005 A Sharkovskii-type theorem for minimally forced interval maps *Topol. Methods Nonlinear Anal.* **26** 163–88
[FKP06] Feudel U, Kuznetsov S and Pikovsky A 2006 Strange nonchaotic attractors *Dynamics between Order and Chaos in Quasiperiodically Forced Systems World Scientific Series on Nonlinear science. Series A: Monographs and Treatises vol 56* (Singapore: World Scientific)

[Fuh16a] Fuhrmann G 2016 Non-smooth saddle-node bifurcations I: existence of an SNA *Ergod. Theor. Dynam. Syst.* **36** 1130–55
[Fuh16b] Fuhrmann G 2016 Non-smooth saddle-node bifurcations III: strange attractors in continuous time *J. Differ. Equ.* **261** 2109–40
[FJR22] Remo F, Fuhrmann G and Jaeger T On the probability of positive finite-time Lyapunov exponents on strange non-chaotic attractors (arXiv:2210.15292)
[Fur61] Furstenberg H 1961 Strict ergodicity and transformation of the torus *Am. J. Math.* **83** 573–601
[GJ13] Gröger M and Jäger T 2013 Dimensions of attractors in pinched skew products *Commun. Math. Phys.* **320** 101–19
[GJT13] Guttal V, Jayaprakash C and Tabbaa O P 2013 Robustness of early warning signals of regime shifts in time-delayed ecological models *Theor. Ecol.* **6** 271–83
[Gle02] Glendinning P 2002 Global attractors of pinched skew products *Dyn. Syst.* **17** 287–94
[GOPY84] Grebogi C, Ott E, Pelikan S and Yorke J A 1984 Strange attractors that are not chaotic *Physica* D **13** 261–8
[HP06] Haro A and Puig J 2006 Strange non-chaotic attractors in Harper maps *Chaos* **16**
[Her83] Herman M 1983 Une méthode pour minorer les exposants de Lyapounov et quelques exemples montrant le caractère local d'un théorème d'Arnold et de Moser sur le tore de dimension 2 *Comment. Math. Helvetici* **58** 453–502
[HY09] Huang W and Yi Y 2009 Almost periodically forced circle flows *J. Funct. Anal.* **257** 832–902
[Jäg03] Jäger T 2003 Quasiperiodically forced interval maps with negative Schwarzian derivative *Nonlinearity* **16** 1239–55
[Jäg07] Jäger T 2007 On the structure of strange non-chaotic attractors in pinched skew products *Ergod. Theor. Dynam. Syst.* **27** 493–510
[Jäg09] Jäger T 2009 The creation of strange non-chaotic attractors in non-smooth saddle-node bifurcations *Mem. Am. Math. Soc.* **945** 1–106
[JS06] Jäger T and Stark J 2006 Towards a classification for quasiperiodically forced circle homeomorphisms *J. London Math. Soc.* **73** 727–44
[K11] Kuehn C 2011 A mathematical framework for critical transitions: bifurcations, fast-slow systems and stochastic dynamics *Physica* D **240** 1020–35
[Kel96] Keller G 1996 A note on strange nonchaotic attractors *Fundam. Math.* **151** 139–48
[KGB+14] Kéfi S *et al* 2014 Early warning signals of ecological transitions: methods for spatial patterns *PLoS One* **9** e92097
[LKK+15] Lindner J F, Kohar V, Kia B, Hippke M, Learned J G and Ditto W L 2015 Strange nonchaotic stars *Phys. Rev. Lett.* **114** 054101
[MCA15] Mitsui T, Crucifix M and Aihara K 2015 Bifurcations and strange nonchaotic attractors in a phase oscillator model of glacial-interglacial cycles *Physica* D **306** 25–33
[NO07] Núñez C and Obaya R 2007 A non-autonomous bifurcation theory for deterministic scalar differential equations *Discrete Contin. Dyn. Syst.* B **9** 701–30
[RBO+87] Romeiras F J, Bondeson A, Ott E, Antonsen T M Jr and Grebogi C 1987 Quasiperiodically forced dynamical systems with strange nonchaotic attractors *Physica* D **26** 277–94
[RDB+16] Olde Rikkert M G M *et al* 2016 Slowing down of recovery as generic risk marker for acute severity transitions in chronic diseases *Crit. Care Med.* **44** 601–6
[RRM15] Rizwana R and Raja Mohamed I 2015 Investigation of chaotic and strange nonchaotic phenomena in nonautonomous wien-bridge oscillator with diode nonlinearity *Nonlinear Dyn.*
[SBB+09] Scheffer M *et al* 2009 Early-warning signals for critical transitions *Nature* **461** 53–9
[Sch09] Scheffer M 2009 *Critical Transitions in Nature and Society* (Princeton, NJ: Princeton University Press)
[SCL+12] Scheffer M *et al* 2012 Anticipating critical transitions *Science* **338** 344–8
[SS00] Stark J and Sturman R 2000 Semi-uniform ergodic theorems and applications to forced systems *Nonlinearity* **13** 113–43
[Sta03] Stark J 2003 Transitive sets for quasi-periodically forced monotone maps *Dyn. Syst.* **18** 351–64
[VFD+12] Veraart J, Faassen J, Dakos V, van Nes H van, Lürling M and Scheffer M 2012 Recovery rates reflect distance to a tipping point in a living system *Nature* **481** 357

[VLPR00] Venkatesan A, Lakshmanan M, Prasad A and Ramaswamy R 2000 Intermittency transitions to strange nonchaotic attractors in a quasiperiodically driven Duffing oscillator *Phys. Rev.* E **61** 3641

[vLWC+14] van de Leemput I A *et al* 2014 Critical slowing down as early warning for the onset and termination of depression *Proc. Natl Acad. Sci. USA* **111** 87–92

[vNS12] van Nes E H and Scheffer M 2007 Slow recovery from perturbations as a generic indicator of a nearby catastrophic shift *Am. Natural.* **169** 738–47

[WFP97] Witt A, Feudel U and Pikovsky A 1997 Birth of strange nonchaotic attractors due to interior crisis *Physica* D **109** 180–90

[Zha13] Zhang Y 2013 Strange nonchaotic attractors with Wada basins *Physica* D **259** 26–36